WESTINGHOUSE NON-PROPRIETARY CLASS 3

WCAP-14708 Revision 1

MODEL 51 STEAM GENERATOR LIMITED TUBE SUPPORT PLATE DISPLACEMENT ANALYSIS FOR DENTED OR PACKED TUBE TO TUBE SUPPORT PLATE CREVICES

APRIL 1997

WESTINGHOUSE ELECTRIC CORPORATION
NUCLEAR SERVICES DIVISION
P. O. BOX 158
MADISON, PENNSYLVANIA 15663-0158

© 1997 Westinghouse Electric Corporation
All Rights Reserved

9706040127 970530
PDR ADOCK 05000275
P PDR

Model 51 SG Limited TSP Displacement Analyses for Dented or Packed Tube to TSP Crevices

Table of Contents

SECTION		PAGE
1.0	INTRODUCTION	1-1
10.0	TSP STRESSES UNDER DENTED CONDITIONS	10-1
10.1	Introduction	10-1
10.2	General Methodology for Detailed Evaluation	10-1
10.3	Detailed Finite Element Models	10-2
10.4	Development of Equivalent Plate Properties	10-3
10.5	Global Finite Element Model	10-4
10.6	Aalysis Cases Considered	10-4
10.7	Tube / Plate Interaction Forces	10-5
10.8	Plate Stresses	10-6
10.9	Weld Stresses	10-8
10.10	Analysis Conclusions	10-10

1.0 INTRODUCTION

This report describes a generic Model 51 steam generator (SG) assessment for limited tube support plate (TSP) displacements in a postulated main steamline break (SLB) event. It is assumed that the SGs evaluated have TSP corrosion as demonstrated by the presence of some denting at TSP intersections. The tube to TSP contact forces resulting from packed crevices with TSP corrosion prevent displacement of the TSP during accident conditions and effectively "lock" the tubes to the TSP. Changes in operating conditions between cold shutdown and full power operation result in the largest temperature differences between the tubes and the tube support structures. Section 10 of Revision 0 of this report provided results of an initial analysis to assess the temperature effects on tube to TSP loads and stresses in the TSPs and support structures. It also indicated in Section 10 that additional work was in progress relative to plate stresses, and that a revision to the report would be issued upon completion of the stress analysis. This report revision, then, provides a summary of the additional analyses to assess the temperature effects on tube to TSP loads and stresses in the TSPs and support structure. The results are documented as an updated Section 10.

10.0 TSP STRESSES UNDER DENTED CONDITIONS

10.1 Introduction

With dented or packed tube to TSP crevices, the tube support plates will experience bending stresses near the wedge and tierod locations when cycling between full power and cold shutdown conditions. If it is assumed that the tube to plate crevices become packed while at full power conditions, then the tubes will impose a downward load on the plates due to differential thermal expansion effects when cycling between different operating regimes. The most significant temperature swings occur when cycling between full power and cold shutdown. Since the TSP displacement analysis relies on the integrity of the tube support plates, and on a tight tube / plate interface, calculations have been performed to determine the degree to which the plates are loaded as a result of the thermal cycling.

In Revision 0 of the WCAP, results were reported for calculations that were performed using the finite element model developed in Section 8.0 for the dynamic analysis. A summary of the results of those calculations is provided in Section 10 of Revision 0. Based on a review of those results, it was concluded that the dynamic model does not provide sufficient detail in the vicinity of the wedge locations to calculate the tube / plate interface forces or the plate stresses. In order to predict the tube / plate interaction and the plate / wedge interaction, an analysis has been performed using detailed models in the wedge and tierod regions. The results of those calculations follow.

10.2 General Methodology for Detailed Evaluation

The finite element model used for the dynamic analysis of the plates is the starting point for the detailed evaluation. However, in the regions adjacent to the wedges and the central tierod, a finer mesh is used. In order to define equivalent plate properties in these regions, a separate model is developed for each area, and corresponding properties determined. The dynamic model is then modified to include more detailed modeling in the wedge and central tierod areas.

Once the model has been modified, the thermal gradient is applied to the model, and plate / tube interaction forces calculated. For any location where the tube / plate breakaway force is exceeded, the tube / plate interface is de-coupled, and the thermal solution rerun. This process is continued until a converged solution is reached, i.e. all tube / plate interface forces are less than the breakaway value.

As was done for the dynamic analysis, two sets of boundary conditions are evaluated. One set corresponding to the support locations in Quadrants 1 and 3 of Figures 8-3 and 8-4, and the second set corresponding to the support conditions in Quadrants 2 and 4 of those same figures. In order to maximize the temperature effects, the calculations are performed assuming hot leg temperature values for the tubes. A summary of the component temperatures used in performing the calculations is provided in Table 10-1.

Since full power operation effectively represents the stress-free condition for this case, it was desirous to have the structure contract from the full power temperature condition to cold conditions. For purposes of this calculation only, negative coefficients of thermal expansion were defined for the materials, which effectively causes a contraction in going from cold shutdown to full power conditions. This allowed the proper reference temperature (70°F) to be maintained, and the proper thermal gradient to be calculated for determining the differential thermal expansions.

10.3 Detailed Finite Element Models

In order to develop equivalent plate properties for the detailed models, separate finite element models are made for each region. The areas of the plate to be modeled, and the number of tube rows / columns included in each model are shown in Figures 10-1 and 10-2. (Note that the wedge and vertical bar shown in Figure 10-2 actually occur in Quadrants 2 and 4 for Plates 2 - 7. It is shown in Quadrant 1 to be consistent with the finite element model.) Three regions are shown in Figure 10-1 corresponding to the wedges located at the [ ]^{a,c} positions, and the area adjacent to the central tierod. The wedges shown at the plate periphery are for the top plate, where the wedge groups are [ ]^{a,c} wide (in the azimuthal direction). For the lower plates, the wedge groups are [ ]^{a,c} in width, with the center of the wedge groups at the same angular position as for the [ ]^{a,c} wedges. Shown in Figure 10-2 is the region in the vicinity of the wedge at the [ ]^{a,c} position, and the vertical bar support at the [ ]^{a,c} position.

Geometry plots of the detailed finite element models for each of these regions are shown in Figures 10-3 through 10-6. In each case, the models include the plates and the interfacing tubes. The models also include the appropriate flow holes, and in the case of the central tierod model, the plate cutout along the tubelane is also included. The models also include a row of elements around each tube corresponding to the corrosion products that cause the tubes to be held in place. These elements were included in the model development so as to permit possible future evaluation of the radial tube / plate interface, but were not included as part

of this evaluation. Instead, for this evaluation, the tube vertical displacements were coupled to the hole boundaries at each interfacing node.

10.4 Development of Equivalent Plate Properties

In order to develop equivalent plate properties for the detailed regions, an equivalent plate model was developed for each region having exactly the same outside geometry, and including the exact same number of tubes. The equivalent plate model for the wedge region in the vicinity of the [ ]^{a,c} wedge is shown in Figure 10-7. For the equivalent plate models, the tubes are included as beam elements, and coupled to the plate in all six degrees of freedom.

A differential thermal expansion was then applied to the tubes in both the detailed and equivalent plate models, and the axial (membrane) stress calculated for each tube in both models. Since the axial force in the tubes is the primary focus of the thermal gradient evaluation, comparison of the axial stress in the two models was judged to be the best measure of whether the equivalent plate models were accurately representing the actual plate response. Based on the results documented in Revision 0 of the WCAP, the differential displacement between the central region of the plate (away from the tierod) and the plate / wrapper interface was [ ]^{a,c} inch. Thus, a temperature gradient was applied to the tubes, for both the detailed and equivalent plate model, that would result in a shrinkage of the tubes of [ ]^{a,c} inch.

In order to compare the results of the two models, a comparative plot of the axial stress in the tubes was generated. The arbitrary numbering scheme used for generating the plots is shown in Figure 10-8 . An iterative process was used, varying two properties of the equivalent plate model, [

]^{a,c}

Thus, [ ]^{a,c} were varied until the axial stresses in the tubes in the equivalent plate model closely matched the results for the detailed model. Plots comparing the axial stresses for the wedge region at [ ]^{a,c} are shown in Figures 10-9, 10-10, and 10-11, for cases corresponding to a [ ]^{a,c} interface with the wrapper. These results show that the equivalent plate model

closely approximates the detailed model in terms of tube axial stress. This same process was repeated for the other detailed models, and similar results were obtained.

10.5 Global Finite Element Model

The revised global model, which includes the channel head, shell, wrapper, tubesheet, tierods and spacers, seven tube support plates, and a large number of tubes is shown in Figure 10-12. Although it is difficult to visualize model details in this figure, it does provide a sense of the density of tubes included in the model. An enlarged view of the top two support plates is provided in Figure 10-13. Model details are more visible in this figure. In addition to the increased detail in the wedge and central tierod regions, two additional model changes from the dynamic model are 1) extending the shell the full height of the tube bundle, and 2) including a tube group representation at essentially every node in the central plate region, instead of the larger tube groupings used in the dynamic model. A plot of the overall model without the tube elements present is shown in Figure 10-14. A plan view plot of the tube support plate is shown in Figure 10-15.

It should be noted in Figure 10-15, that based on the analysis of the detailed model regions, the detailed areas in the global model are increased in size relative to the detailed models. The areas were increased in size in order to provide a larger area for load attenuation between the wedge area and the central region of the plate. A comparison of the size of the model refinement in the global and detailed models is provided in Figures 10-16 and 10-17. The size of the detailed models is outlined with a solid line, while the amount of area included in the global model refinement is delineated by the areas where tubes are shown.

Overall, the global model includes [
]^{a,c} of the tubes in the modeled region. The remaining tubes are included in [ ]^{a,c} tube groups.

10.6 Analysis Cases Considered

As discussed above, and in Sections 8.3 and 8.4 of Revision 0, solutions are obtained for two sets of wedge arrangements. The first solution is for the wedge arrangement in Quadrants 1 and 3 of Figures 8-3 and 8-4, and the second solution for the wedge arrangement in Quadrants 2 and 4. In addition, two different interfaces are assumed between the plate and wrapper. For the first case, the plate and wrapper motions are coupled in all six degrees of freedom. For the

second case, the plate and wrapper motions are coupled in translational degrees of freedom only.

Finally, both minimum and maximum breakaway forces are considered. Based on the Dampiere-1 data and $\pm\sigma$ variation about the average breakaway force of 2686 pounds, the minimum and maximum breakaway forces are 1630 and 3740 pounds, respectively.

Overall, there are eight cases to be considered as part of the analysis.

10.7 Tube / Plate Interaction Forces

The first cases considered in the analysis are for the minimum breakaway force. The results for those cases show all the plate / tube interaction forces to be less than the maximum breakaway force. Thus, there are no tubes predicted to breakaway as a result of exceeding the maximum breakaway force, and the maximum breakaway force cases are satisfied by inspection. Thus, the matrix of cases considered reduces from eight to four.

A plot of the displaced geometry for the Quadrant 1 and 3 wedge support arrangement with the plate and wrapper coupled for all degrees of freedom is shown in Figure 10-18. An enlarged view of the displaced geometry for Plates 6 and 7 is shown in Figure 10-19. These plots show how the peak displacements are concentrated near the plate / wrapper interfaces, and then drop off rapidly with distance away from the support locations. Similar plots for the Quadrant 2 and 4 support arrangement, again with the plate and wrapper coupled for all degrees of freedom, are shown in Figures 10-20 and 10-21, with the same types of displacement patterns.

Summaries of the resulting interface loads for the minimum breakaway cases are provided in Tables 10-2 through 10-5. Tables 10-2 and 10-3 provide the results for the Quadrant 1 and 3 wedge arrangement, with all plate / wrapper degrees-of-freedom coupled in Table 10-2 and the plate / wrapper pinned in Table 10-3. Tables 10-4 and 10-5 provide similar results for the Quadrant 2 and 4 wedge arrangement. Referring to Table 10-2, a summary of the plate / tube interface forces is provided for each plate. The interface forces are grouped by force magnitude to identify the number of tubes with a given force level. The tubes are also grouped by region, Interior, Detail 1, etc. A plot of the tube support plate with the various regions identified is shown in Figure 10-22. Finally, in the far right hand column is the number of "inactive" tubes for each plate and region. This corresponds to the number of tubes where the breakaway force was exceeded.

As the results show, the only plates where the breakaway force is exceeded are Plates [ ]^{a,c}

Plots showing the location of the inactive tubes are provided in Figures 10-23 through 10-27. The results in Tables 10-2 through 10-5 show that there are some slight differences in the results between the cases with the plate / wrapper coupled in all degrees of freedom, and the case where they are pinned only. The tubes identified in Figures 10-23 through 10-27 represent an envelope of the tubes from the two plate / wrapper interface conditions.

Plots showing the distribution of interface forces for the top plate for each of the four cases are provided in Figures 10-28 through 10-31. One thing to note in each of these figures is that there is an increase in the interface force at the transition between the regions of detailed modeling and the interior region where the mesh size is larger. This is, in fact, due to the change in mesh size, and the effective decrease in plate stiffness in these regions. Since the spacing between tubes is now larger, the effective bending stiffness of the tubes and plate is decreased. To improve on the solution would require a separate evaluation, similar to that performed for each of the detailed regions, to define a new set of equivalent plate properties in this region to more closely approximate the combined bending stiffness of the tube and plate. Because these areas are removed form the areas of concern, and because the interface forces have reduced to relatively low values at the edge of the detailed regions, the reduced stiffness of the interior region is not expected to have a significant effect on the wedge regions. Thus, an analysis to improve on the combined tube and plate stiffness in the interior region is not considered necessary.

10.8 Plate Stresses

The concern relative to the plate stresses is one of fatigue and the potential to develop cracks in the vicinity of the wedges or tierods. The functional requirement of the plates is to provide lateral support for the tubes. The plates can satisfy the structural requirement, even with cracks present, so long as the cracks do not form in such a way as to lose a piece of the plate. The formation of cracks in the vicinity of the wedges could also potentially affect the deformation characteristics of the plates under in-plane loading conditions, such as LOCA + SSE, where the loads are reacted through the wedges to the shell. This effort does not address how the in-plane strength of the plates is affected by the presence of cracks in the vicinity of the wedges. Rather, the scope of this effort is limited to an assessment of the potential to develop fatigue cracks as a result of the cyclic loading.

In order to calculate plate stresses in the wedge and tierod regions, the detailed finite element models are used. One method for calculating these stresses is to develop mapping functions that would translate the plate and tube displacements from the global model into boundary conditions at the periphery of the detailed models, which would then be solved to calculate the plate stresses. An alternative method, and the one that is used here, is to apply thermal gradients to the tube elements in the detailed models that approximate the differential displacement between the internal plate regions and the wedge support locations. Conservative, zero rotation, boundary conditions are applied to the edges of the detailed models where they interface with the remainder of the plate. In addition, all tube / plate interfaces are also considered to be active, i.e., no breakaway has occurred. One drawback to this method is that is does not simulate the interfacing stiffness of the wrapper. Overall, with the rotational constraint provided at the edges of the detailed regions, combined with the assumption that all tubes are active, this method is judged to provide a conservative approximation of the plate stresses.

Based on the preliminary work to establish equivalent material properties for the plates, the stresses in the top plate, with the [ ]^{a,c} wedge width are the most limiting. Thus, plate stresses are calculated for the top plate with the [ ]^{a,c} wedge regions. Given that the differential expansion between the tubes and wrapper is also highest for this plate, the stresses for plate 7 are expected to bound the lower plates.

A summary of the differential expansions between the plate / wrapper interface locations and the edge of the corresponding detailed region for the final converged solutions is provided in Table 10-6. Based on these differential displacements, temperature gradients are applied to the tubes that result in a corresponding shrinkage of the tubes. Again, zero edge rotations are specified at the edges of the detailed models, where they interface with the remainder of the plate. Stress contour plots of the top surface stress intensity are shown in Figures 10-32 through 10-36 for each of the support locations. Figures 10-32, 10-33, and 10-34 show the stress intensities for each of the three wedge support locations, [ ]^{a,c}, respectively. Figure 10-35 corresponds to the [ ]^{a,c}, and Figure 10-36 corresponds to the central tierod region.

Except for the central tierod region, significant plate stresses are predicted. The most limiting region is in the vicinity of the wedge at the [ ]^{a,c}. In the course of this analysis, the local stiffness of the plate was found to vary relative to the orientation of the hole pattern with the loading introduced through interaction between the plate and the wrapper. The plate stiffness was found to be lowest for the wedge located at the [ ]^{a,c} position. This is consistent

with the locally high stresses. The peak stresses in the other regions, although high, are significantly lower than for the [ ]^{a,c} position.

Using the applicable ASME Code fatigue curve, an allowable number of cycles for this event is shown summarized in Table 10-7. These results show that for detailed region [ ]^{a,c} years of operation before any cracks would develop. Referring to Figure 10-32, the peak stresses are isolated to two ligaments, with the maximum stresses in the remaining areas being about 30% lower. The allowable number of cycles for the remainder of the region is [ ]^{a,c} years of operation. For the remaining wedge regions, the allowable number of cycles exceeds 1000. The number of cycles defined in the design specifications for this event is 250, so the value of 1000 or more is acceptable. Relative to an overall fatigue usage for the plates, there are no other events that would introduce a significant fatigue loading to the plates. This event is clearly the dominant loading for the plates.

Again, as discussed above, should any localized cracks develop in the plate, the safety function of the plate would not be impaired without loss of a piece of the plate. Given the potential for high fatigue usage predicted by this analysis, it is considered prudent for plants with high levels of dented or packed crevices to include a sampling of tubes in and around the wedge regions for eddy current inspection in order to check for any ligament cracking that might develop. Visual examination of the wedge regions could also be used to look for the presence of cracks. Relative to the in-plane loadings, and potential plate deformation under LOCA+ SSE, should plate cracking be observed, then an analysis can be performed to establish any tubes that might be at risk due to the presence of the cracks.

10.9 Weld Stresses

As with the tube support plates, the concern relative to the weld stresses is one of fatigue. In the case of the plate / wedge welds, however, the ability of the plates to provide lateral support for the tubes, would not be adversely affected by cracks in these welds. Also, the motion of the plates under steam line break loads is not significantly affected by cracks in these welds. The tubes, due to the dented and packed intersections, will continue to hold the plates in place under SLB loads. Thus, there is no structural requirement associated with the integrity of the welds between the plate and wedges. As with the plates, this evaluation is not intended to be an ASME Code evaluation of the welds, which are non-pressure boundary components, but rather an assessment of the potential to develop fatigue cracks as a result of the cyclic loading.

To calculate the weld stresses, nodal forces are extracted from the global model at the plate / wrapper interface, and conventional calculations used to determine the resulting weld stresses. The stresses are calculated for the case where the plate and wrapper are coupled for all degrees of freedom. Since the wedges are welded to the plate on both the top and bottom surfaces (see Figure 8-2), a truly plastic hinge cannot develop. Thus, the resulting moment load is converted to a force couple, and the stresses calculated.

For all of the wedge locations, the plates are coupled to the wrapper at three nodes, corresponding to each end of the wedge and the center position. In calculating the weld stresses, the end node forces are assumed to be reacted by one-fourth of the weld area, and the central node force by one-half of the weld area. Since the wedge width for plates one to six is [ ]^{a,c}, compared to the [ ]^{a,c} wedge width for the top plate, calculations are performed for both plates six and seven. Although the interaction forces for plate six are somewhat smaller than for plate seven, they are reacted by a smaller weld area, and the resulting stresses are higher.

A somewhat different methodology is followed for the weld between the vertical bar support and the plate. As shown in Figure 8-2, the vertical bars are welded only to the bottom of the plates, and therefore are expected to develop a plastic hinge at this location. Thus, for evaluating the vertical bar welds, reaction forces from the case where the plate and wrapper are coupled in translational degrees of freedom only is used.

Using the applicable ASME Code fatigue curve, an allowable number of cycles for this event is shown summarized in Table 10-8. Consistent with the guidelines of the ASME Code for fillet welds, a stress concentration factor of 4.0 is applied to the stress normal to the weld throat, which would tend to open a crack at the root of the weld. Referring to Table 10-8, the limiting number of cycles for the wedge welds is [ ]^{a,c} years of operation. For the vertical bar welds, the limiting number of cycles is [ ]^{a,c}.

As discussed above, both the vertical bar and wedge welds do not have any safety related function. This is particularly true of the vertical bars, which are used to help align the plates during installation. Should any localized cracks develop in the welds, the safety function of the tube support plates plate would not be impaired. The primary function of the tube support plates is to provide lateral support for the tubes. Cracking of the welds between the wedges and tube support plates, or between the vertical support bar and the plate would not impact the ability of the plates to provide lateral support to the tubes.

Cracking of the welds between the wedges and tube support plates should also not have a significant affect on the dynamic response of the plates under SLB loads. Since the wedges have a sloped face, they will continue to resist upward displacement of the plates, which is the direction of the dominant loading for the SLB event.

10.10 Analysis Conclusions

Based on the results of these calculations, the following conclusions are made.

1. A limited number of tubes are predicted to exceed the breakaway force of 1630 pounds in the vicinity immediately adjacent to the wedge regions. Should any localized cracks develop in the plate, the safety function of the plate would not be impaired without loss of a piece of the plate. The tubes that exceed the breakaway force are limited to Plates [ ]^{a,c}. The number of tubes exceeding the breakaway force at particular wedge location is small, [ ]^{a,c} or less, and should not effect the dynamic response of the tube support plates to the Steam Line Break loading.

2. As a result of the thermal cycling load with dented or packed intersections, locally high stresses are predicted to occur in the tube support plates. Given the potential for high fatigue usage predicted by this analysis, it is considered prudent for plants with high levels of dented or packed crevices to include a sampling of tubes in and around the wedge regions for eddy current inspection in order to check for any ligament cracking that might develop. Visual examination of the wedge regions could also be used to look for the presence of cracks. Relative to in-plane loadings, and potential plate deformation under LOCA+ SSE, should plate cracking be observed, an evaluation can be performed to establish any tubes that might be at risk due to the presence of the cracks.

3. As with the tube support plates, thermal cycling with dented or packed intersections, results in potentially high fatigue usage in the welds joining the wedges and the tube support plate, and the welds between the vertical bar supports and the tube support plates. However, cracking of the welds between the wedges and tube support plates, or between the vertical support bar and the plate would not impact the ability of the plates to provide lateral support to the tubes. With the assumption of dented or packed intersections, the dynamic response of the plates under SLB loads should also not be significantly affected by the presence of cracks in these welds. The tubes provide significant restraint to the plates under SLB loads, and would continue to hold plates in place. Thus, cracking of these

welds is concluded to not have a negative consequence relative to the conditions considered as part of the limited displacement analysis.

4.. Since the stress levels in the tube support plate are predicted to exceed yield, the elastically calculated tube / support plate interaction forces are conservative. Local yielding of the plate should relieve the axial force on the tube and hence the tube / plate interaction forces.

Table 10-1

Summary of Component Temperatures
Full Power Conditions

a,c

[ ]

Table 10-2

Summary of Tube / Plate Interface Forces
Quadrant 1, 3 Support Conditions
Plate / Wrapper - All DOF Coupled

a,c

[ ]

Table 10-3

Summary of Tube / Plate Interface Forces
Quadrant 1, 3 Support Conditions
Plate / Wrapper - Pinned Support

a,c

Table 10-4

Summary of Tube / Plate Interface Forces
Quadrant 2, 4 Support Conditions
Plate / Wrapper - All DOF Coupled

a,c

[ ]

Table 10-5

Summary of Tube / Plate Interface Forces
Quadrant 2, 4 Support Conditions
Plate / Wrapper - Pinned Support

a,c

[ ]

Table 10-6

Summary of Differential Displacements
Tube Support Plate / Wrapper Support

a,c

[ ]

Table 10-7

Summary of TSP Allowable Cycles

a,c

[ ]

Table 10-8

Summary of Weld Allowable Cycles

a,c

[ ]

a,c

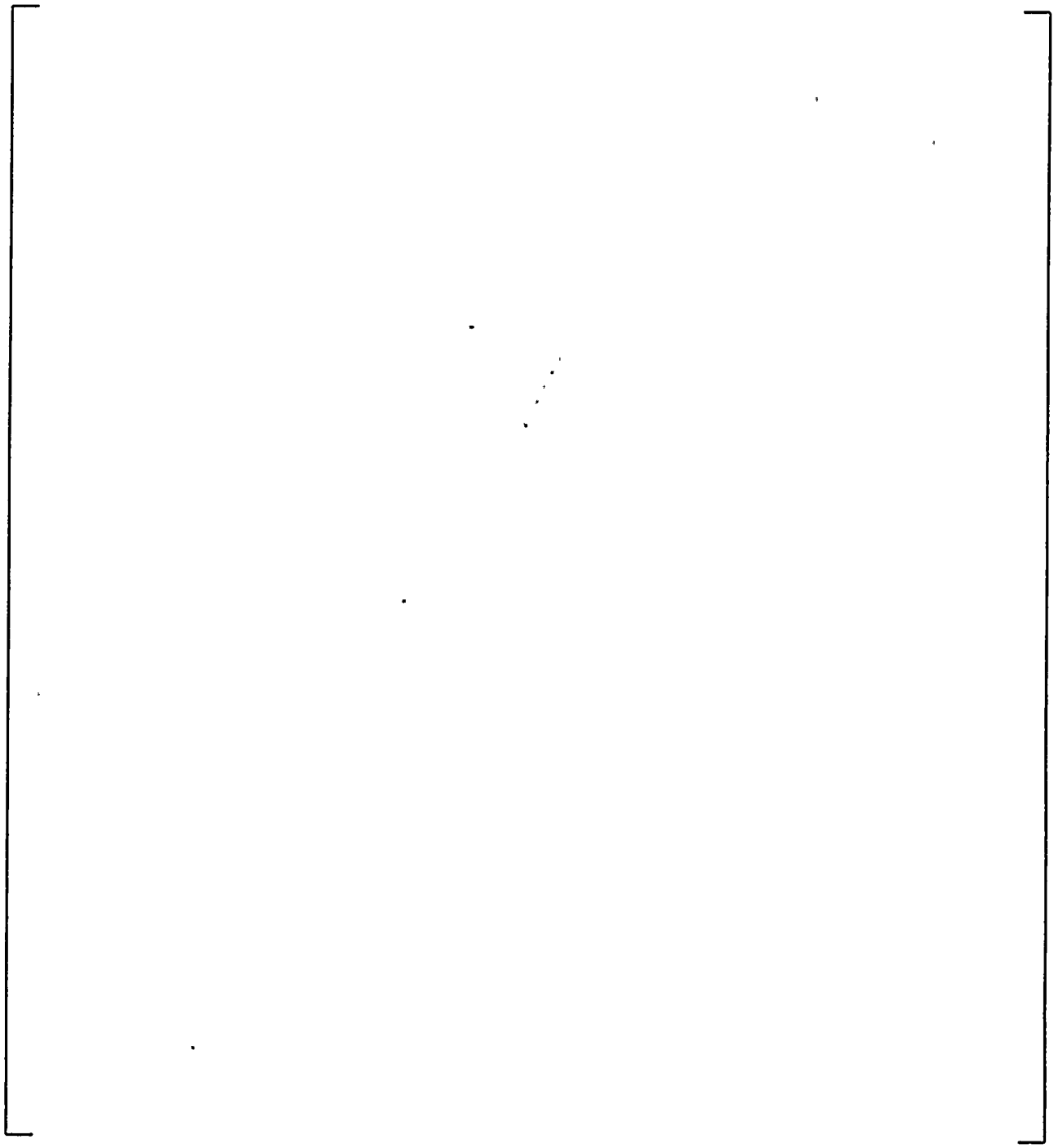

Figure 10-1. Model 51 Tube Support Plate
Location and Size of Detailed Plate Regions
Regions 1, 3, and 4

a,c

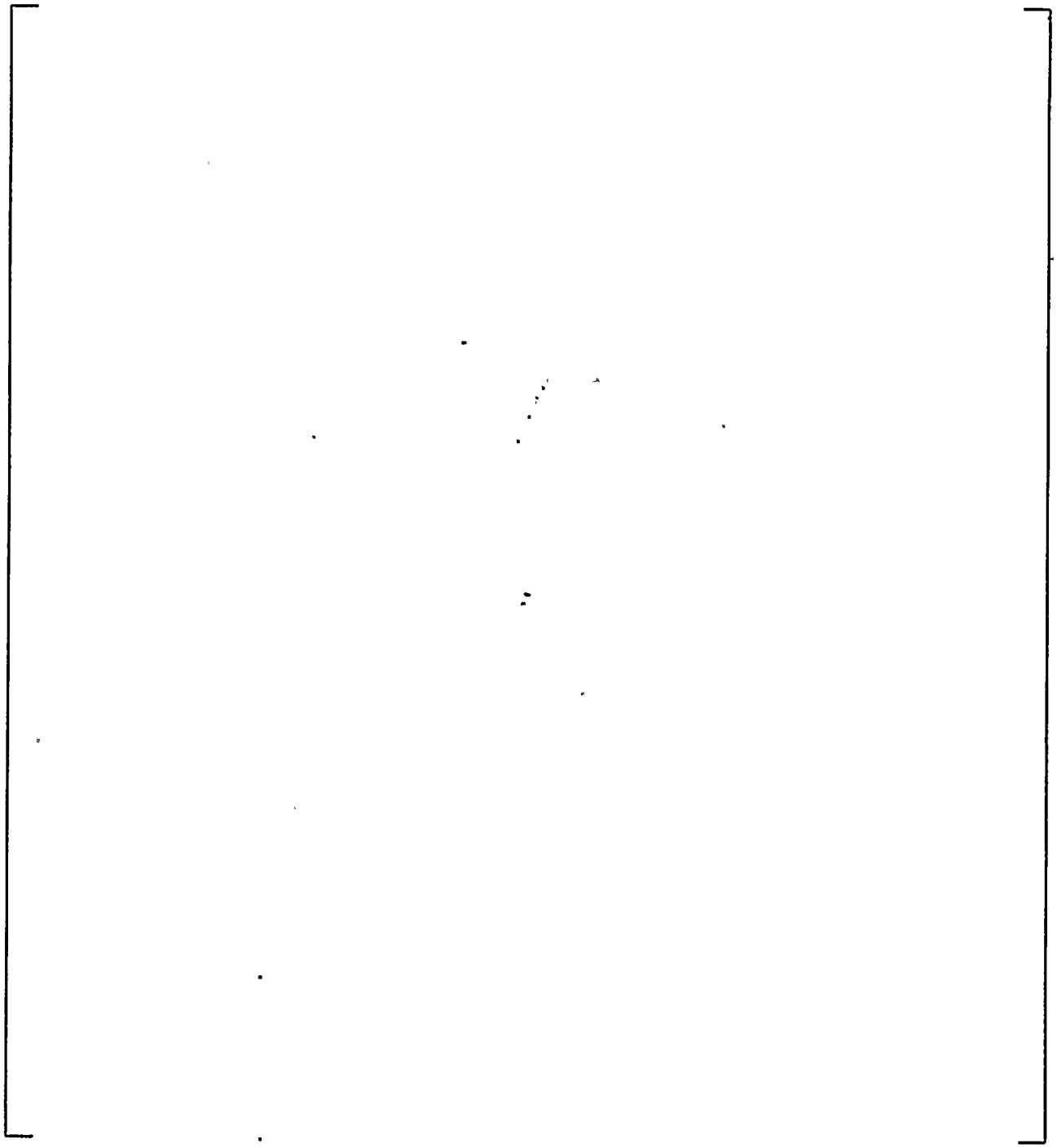

Figure 10-2. Model 51 Tube Support Plate
Location and Size of Detailed Plate Regions
Region 2

a,c

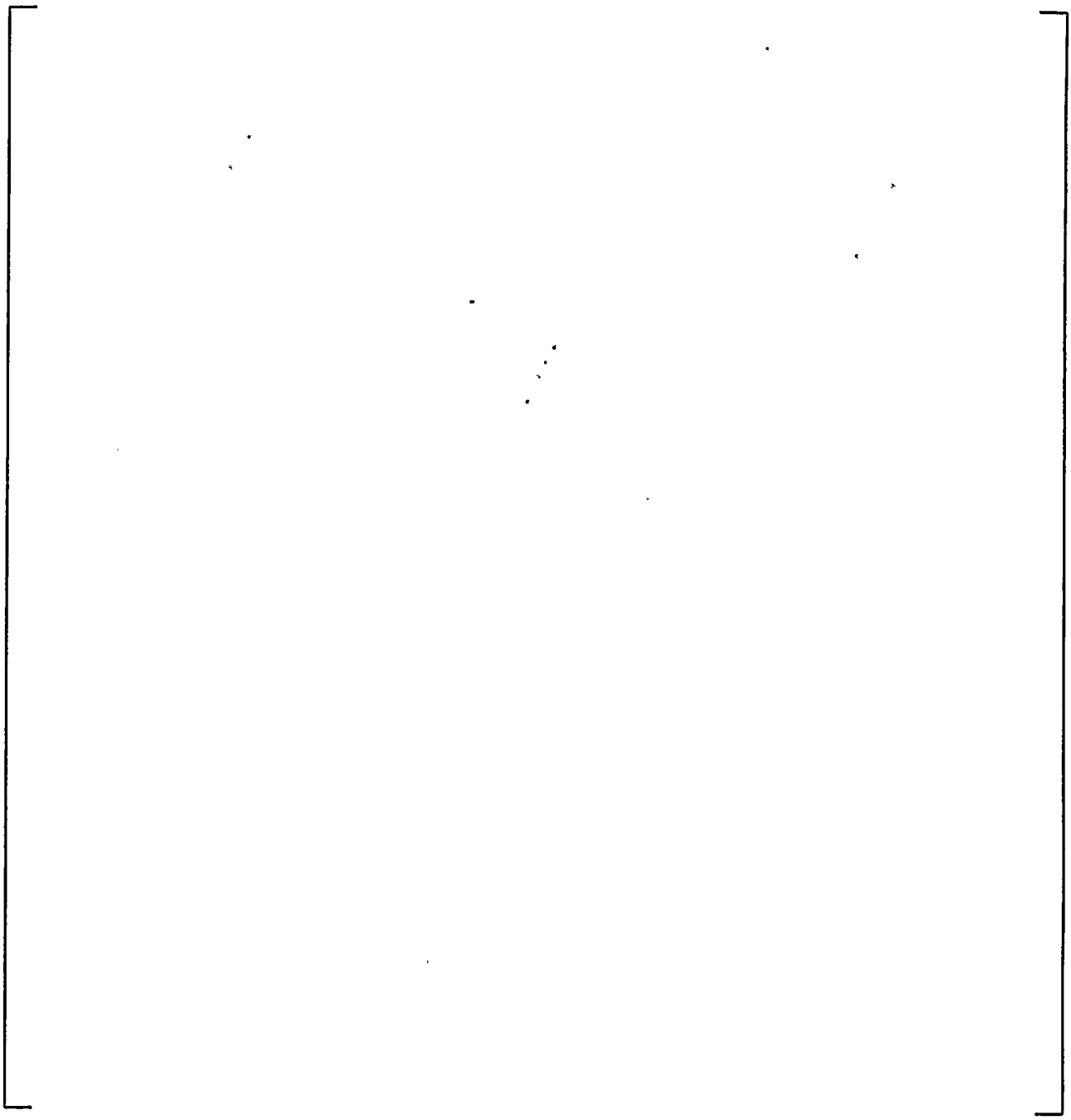

Figure 10-3. Finite Element Model
Detailed Region 1

a,c

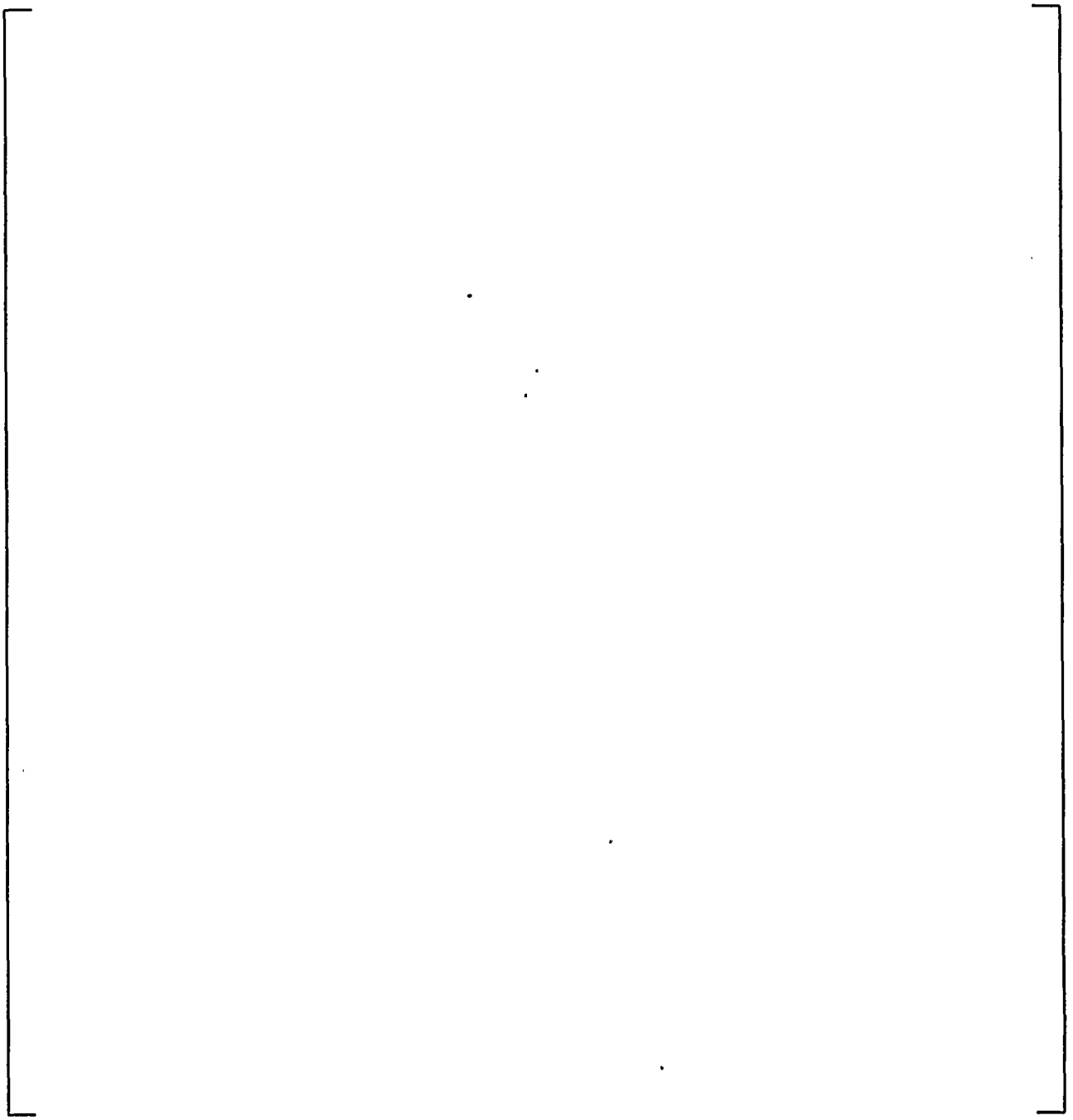

Figure 10-4. Finite Element Model
Detailed Region 2

a,c

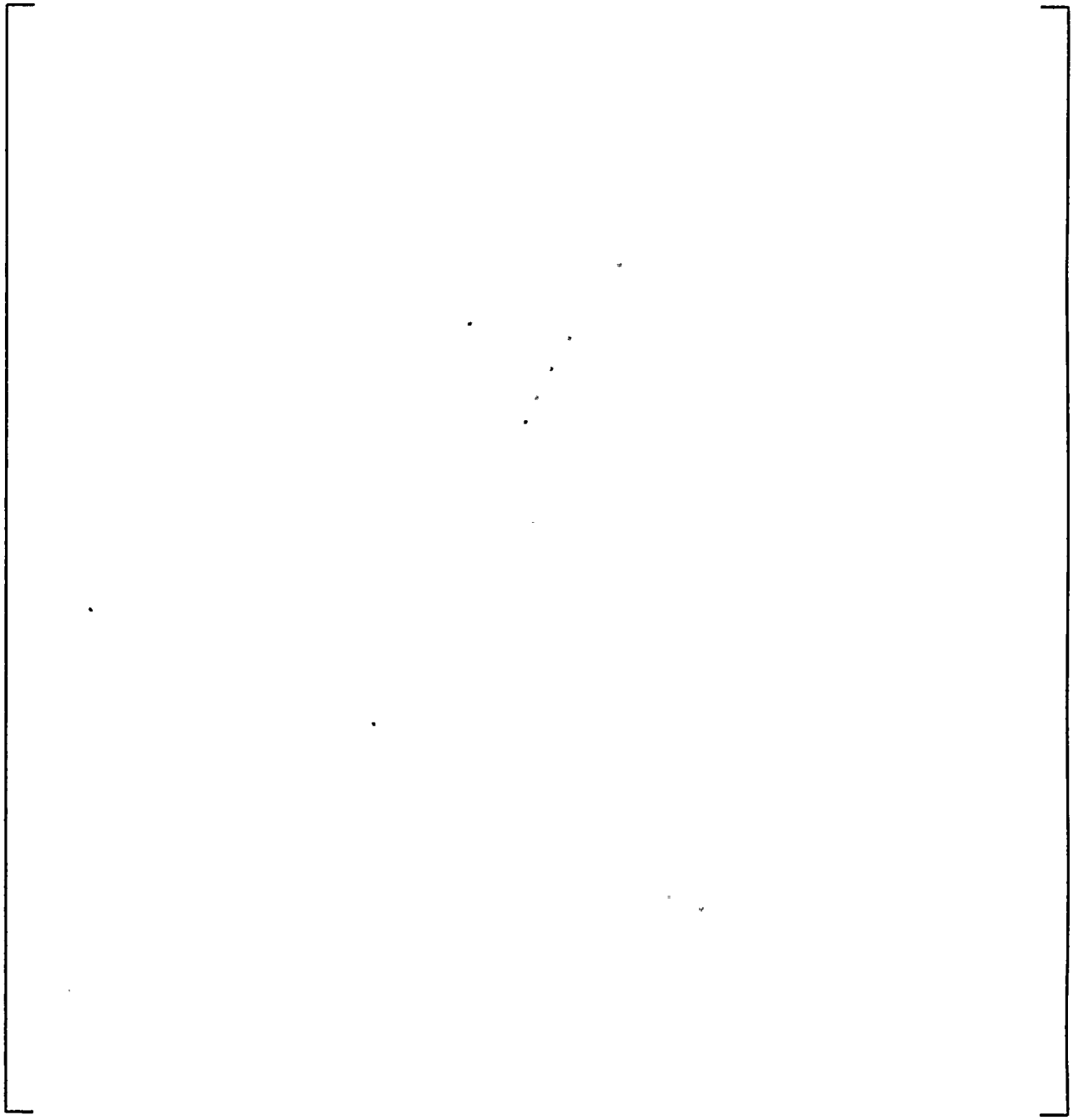

Figure 10-5. Finite Element Model
Detailed Region 3 / Patch Plate

a,c

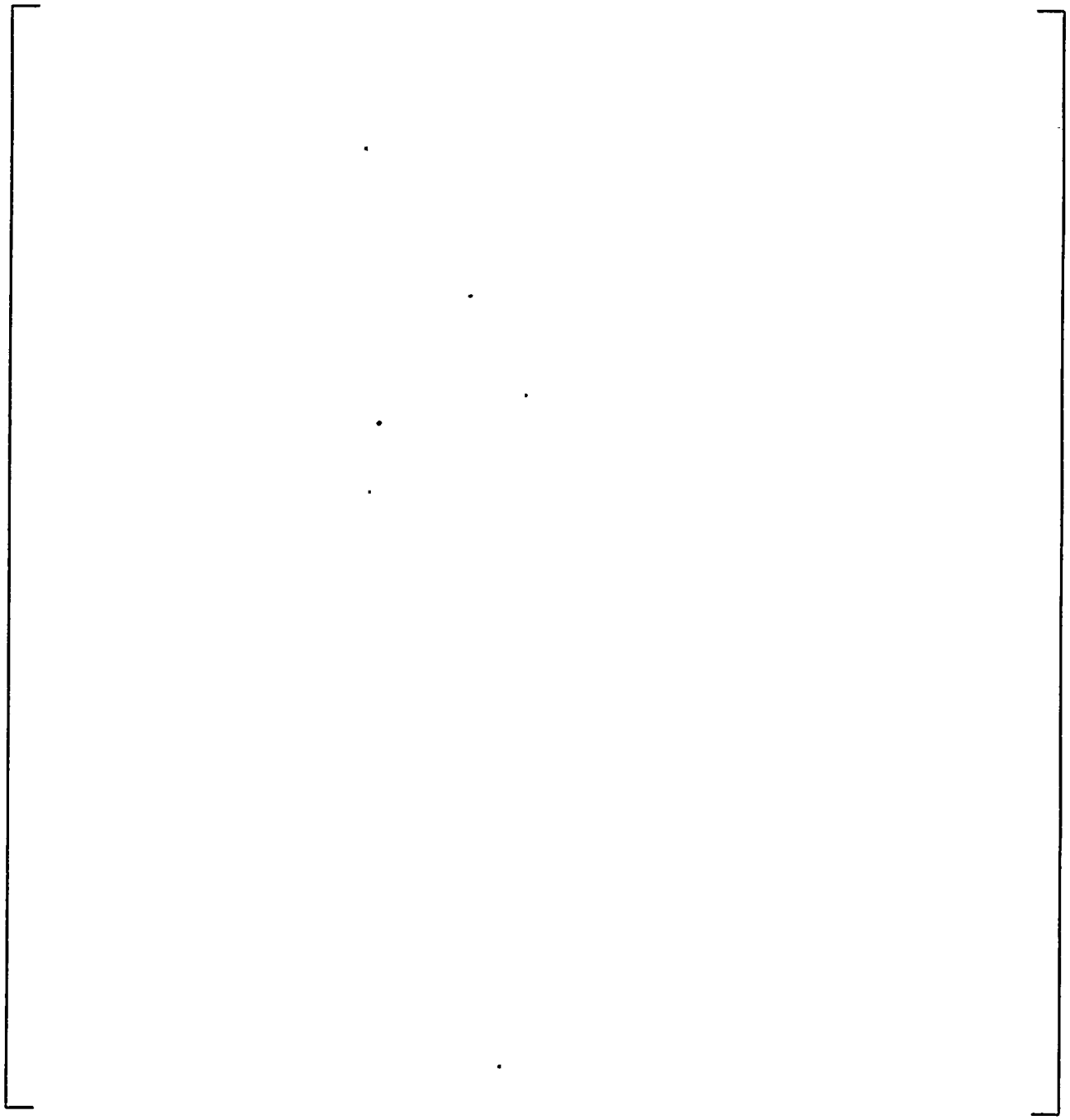

Figure 10-6. Finite Element Model
Detailed Region 4

a,c

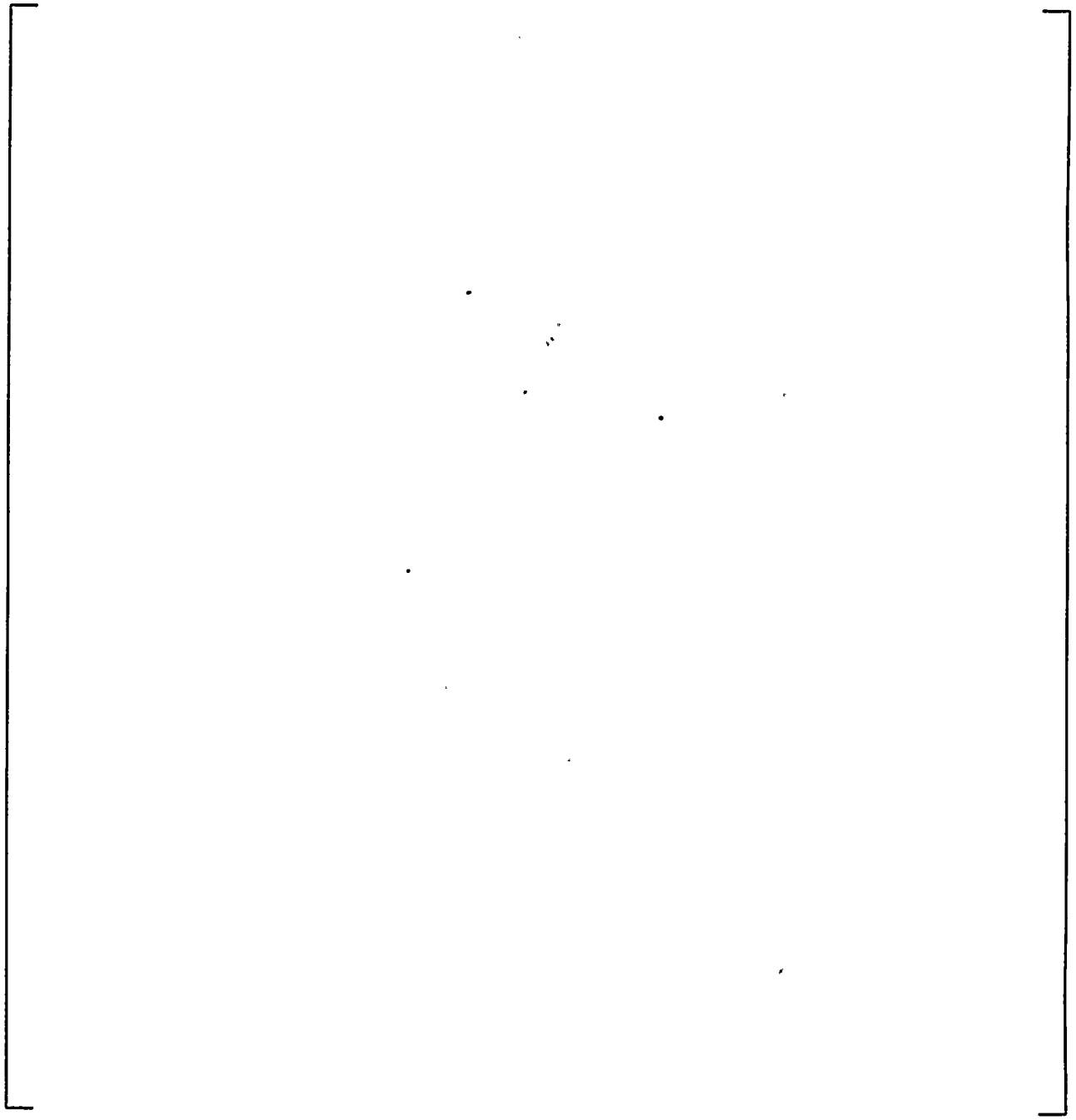

Figure 10-7. Equivalent Plate Finite Element Model Detailed Region 3 / Patch Plate

a,c

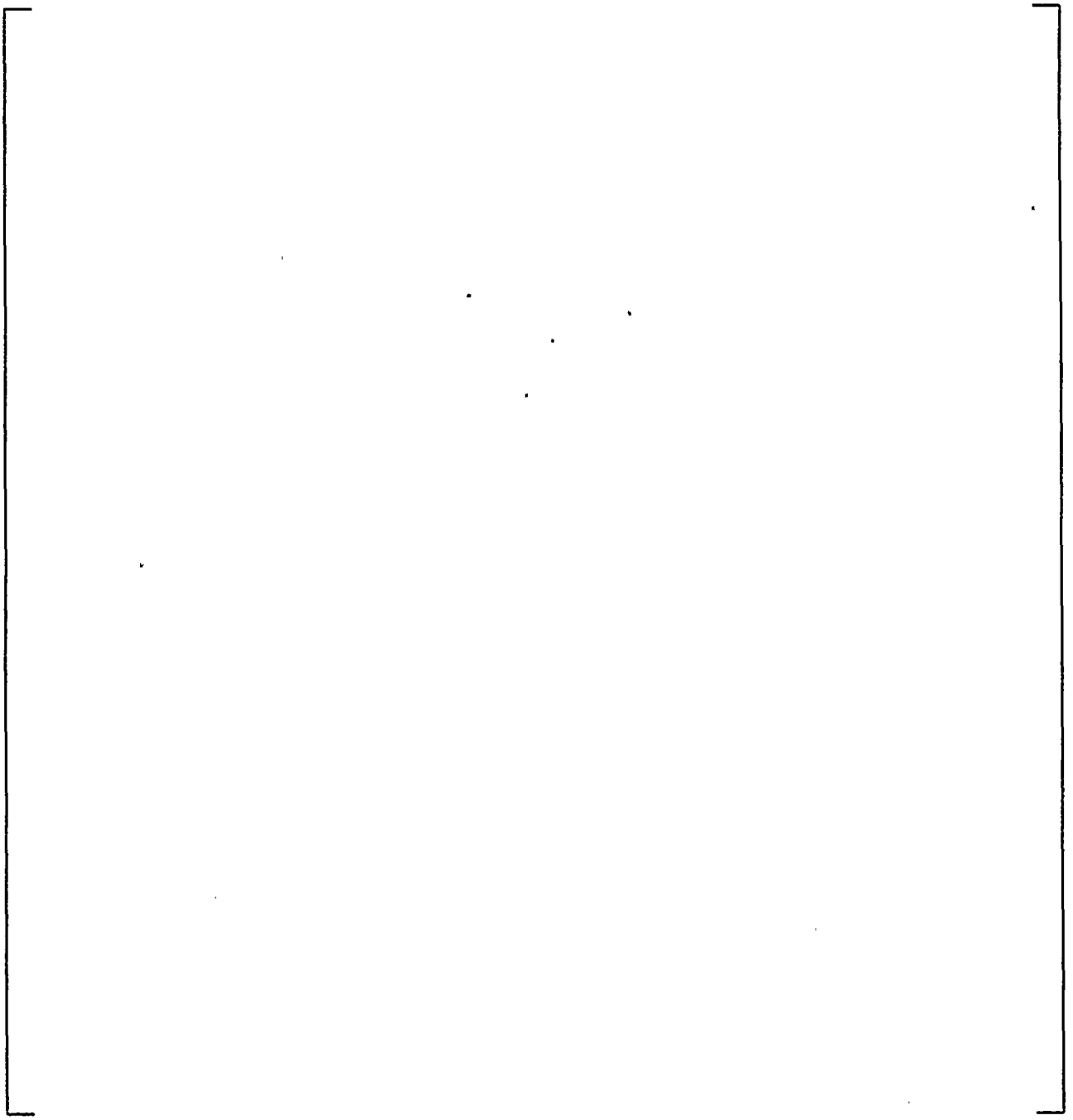

Figure 10-8. Tube Numbering Scheme
Detailed Region 3 / Patch Plate

a,c

Figure 10-9. Comparison of Tube Axial Stress
Detailed Region 3 / Patch Plate
Ten Inch Wedge Width

a,c

Figure 10-10. Comparison of Tube Axial Stress
Detailed Region 3 / Patch Plate
Six Inch Wedge Width

a,c

Figure 10-11. Comparison of Tube Axial Stress
Detailed Region 3 / Patch Plate
One Inch Vertical Bar Support

a,c

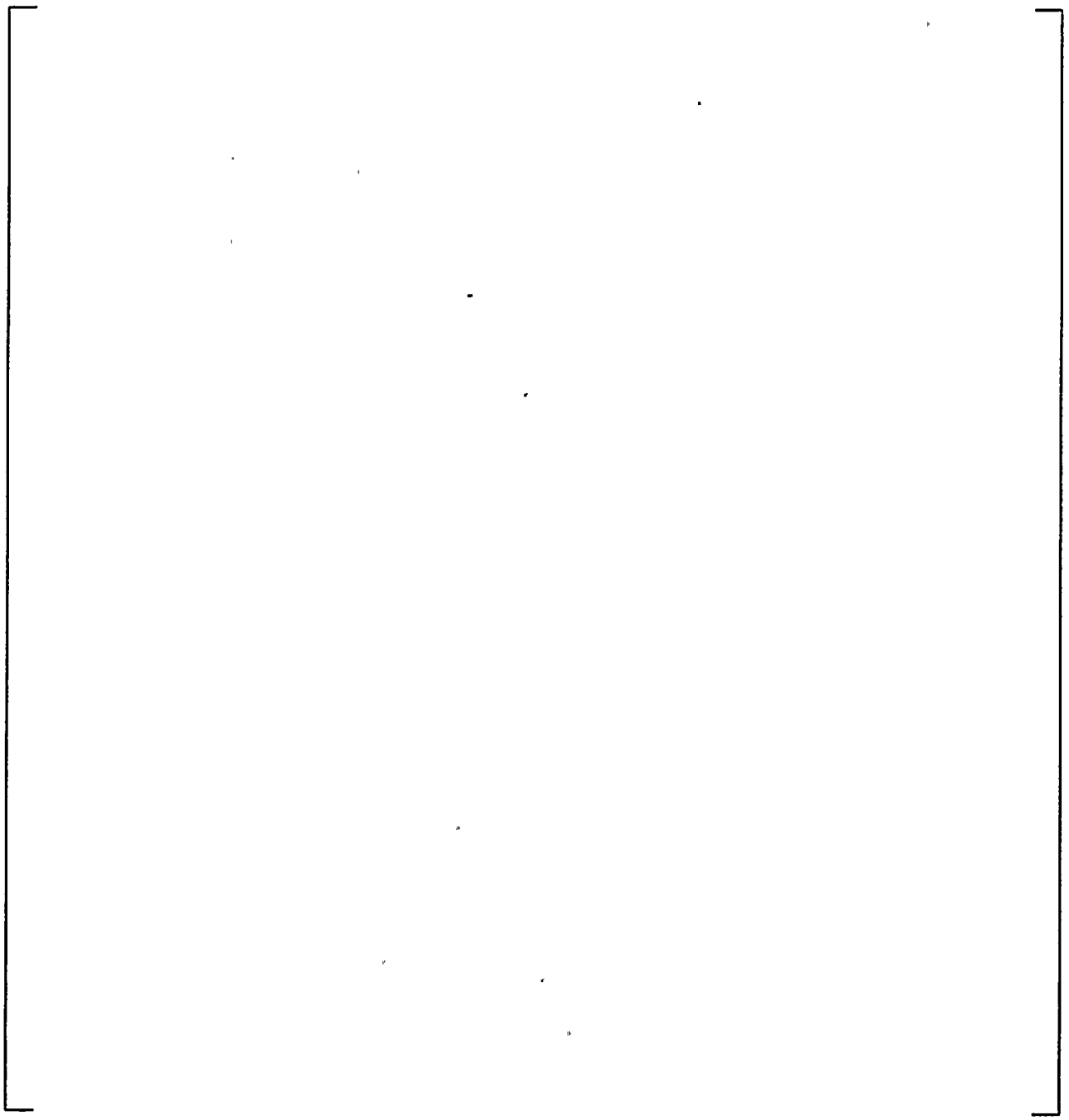

Figure 10-12. Finite Element Model
Revised Global Model

a,c

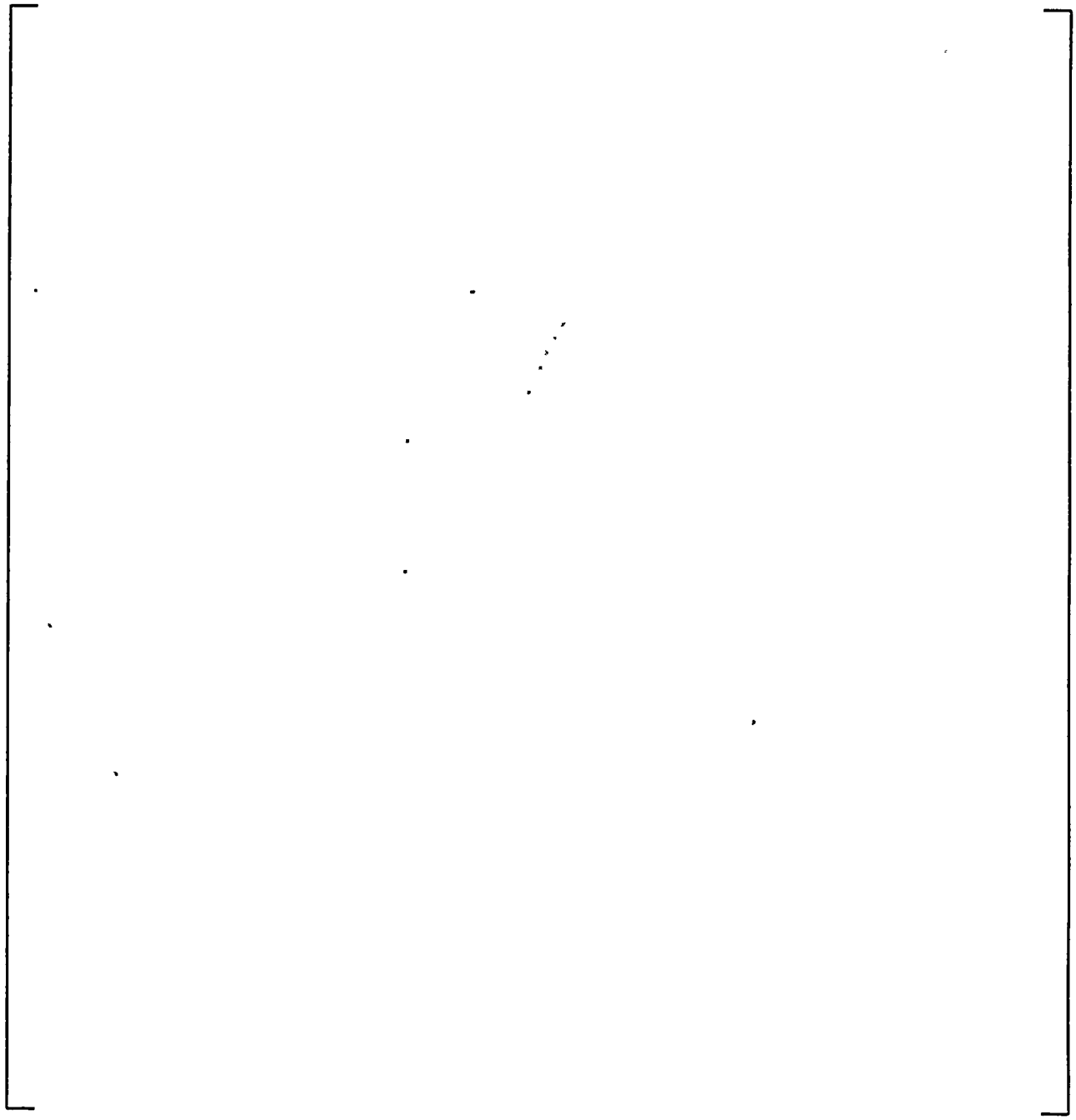

Figure 10-13. Revised Global Model
Enlarged View of TSP 6 and 7

a,c

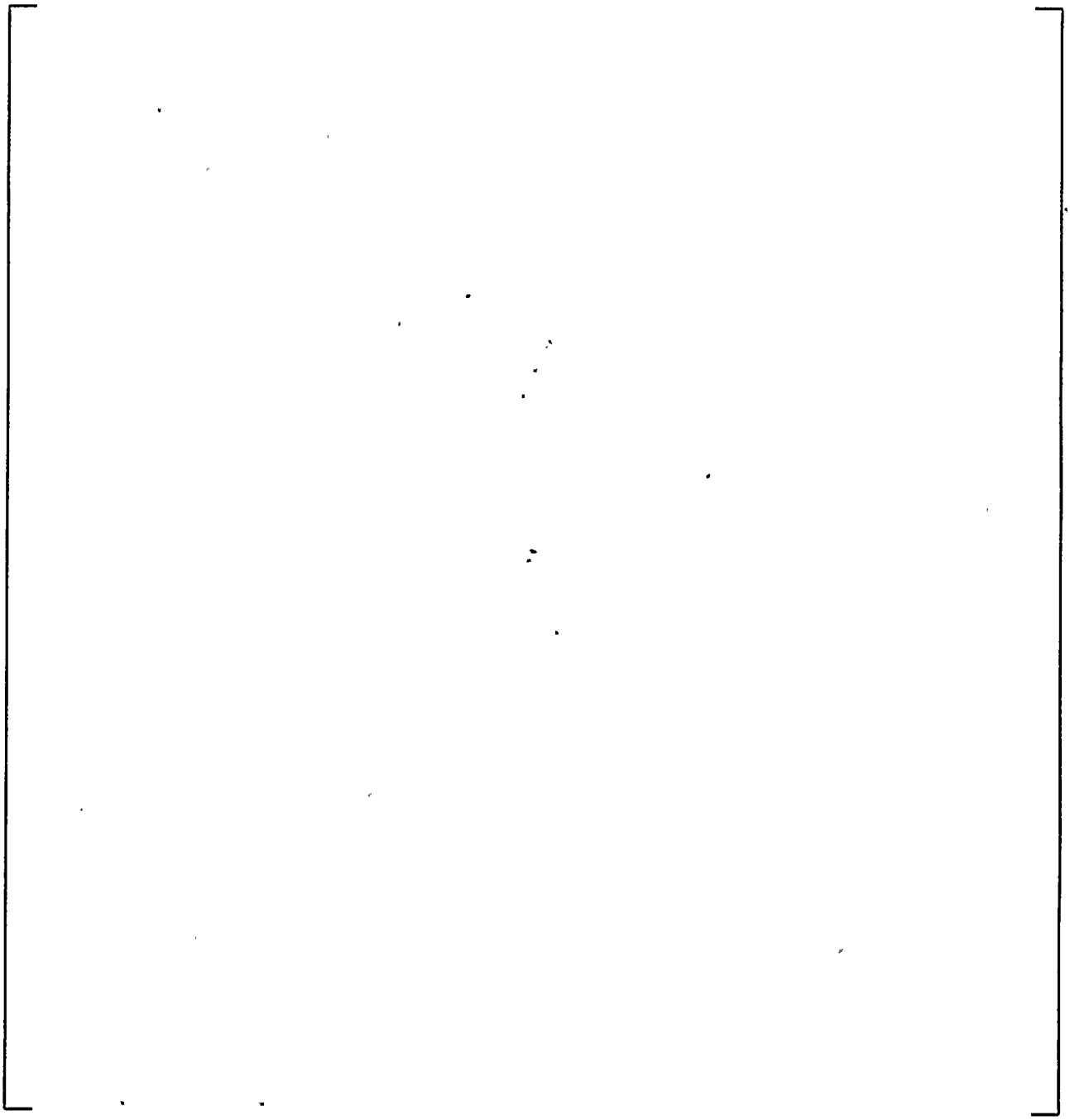

Figure 10-14. Revised Global Model
Tube Elements Not Shown

a,c

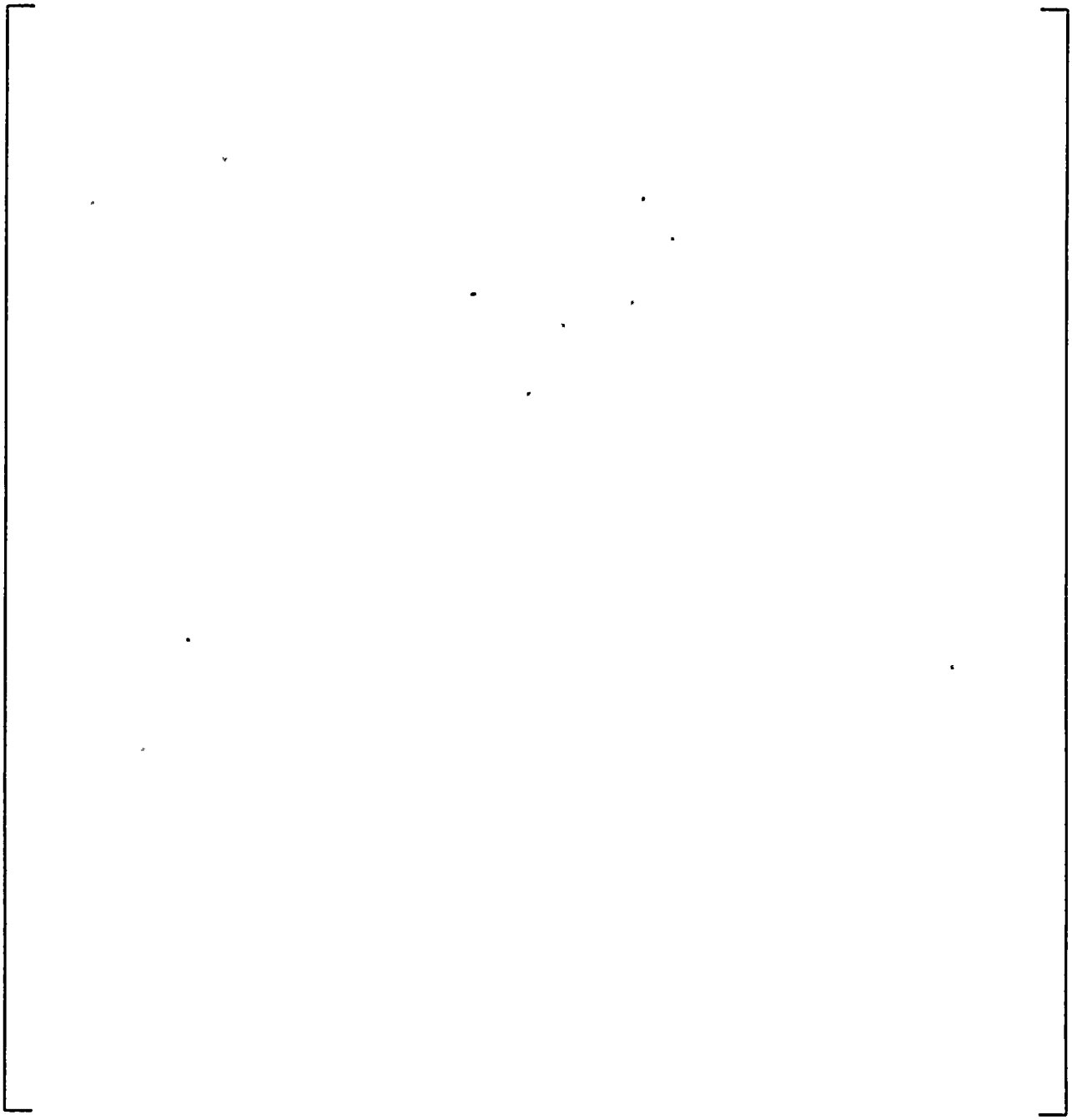

Figure 10-15. Revised Global Model Plan View of Tube Support Plate

a,c

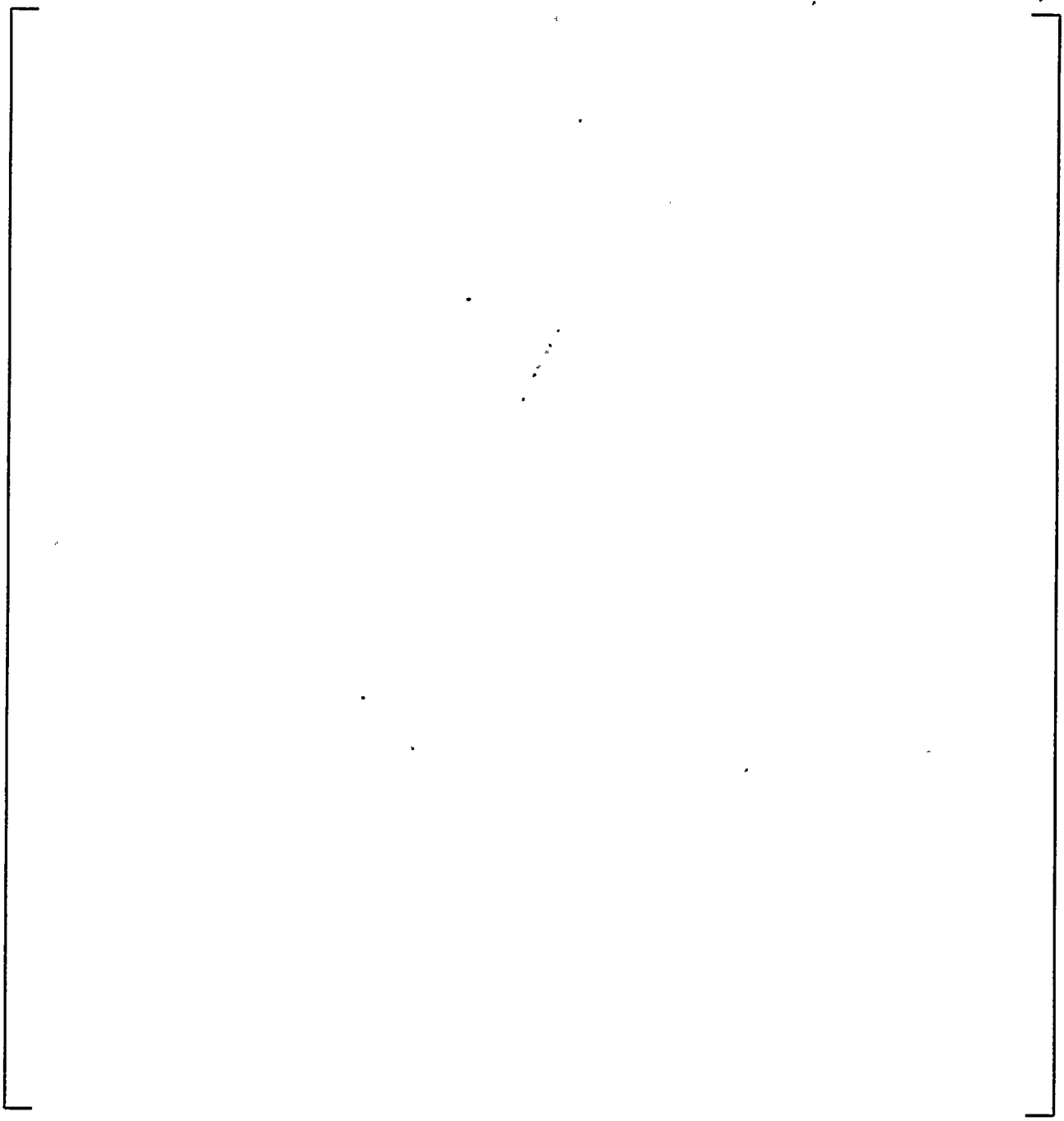

Figure 10-16. Revised Global Model
Location and Size of Detailed Plate Regions
Regions 1, 3, and 4

a,c

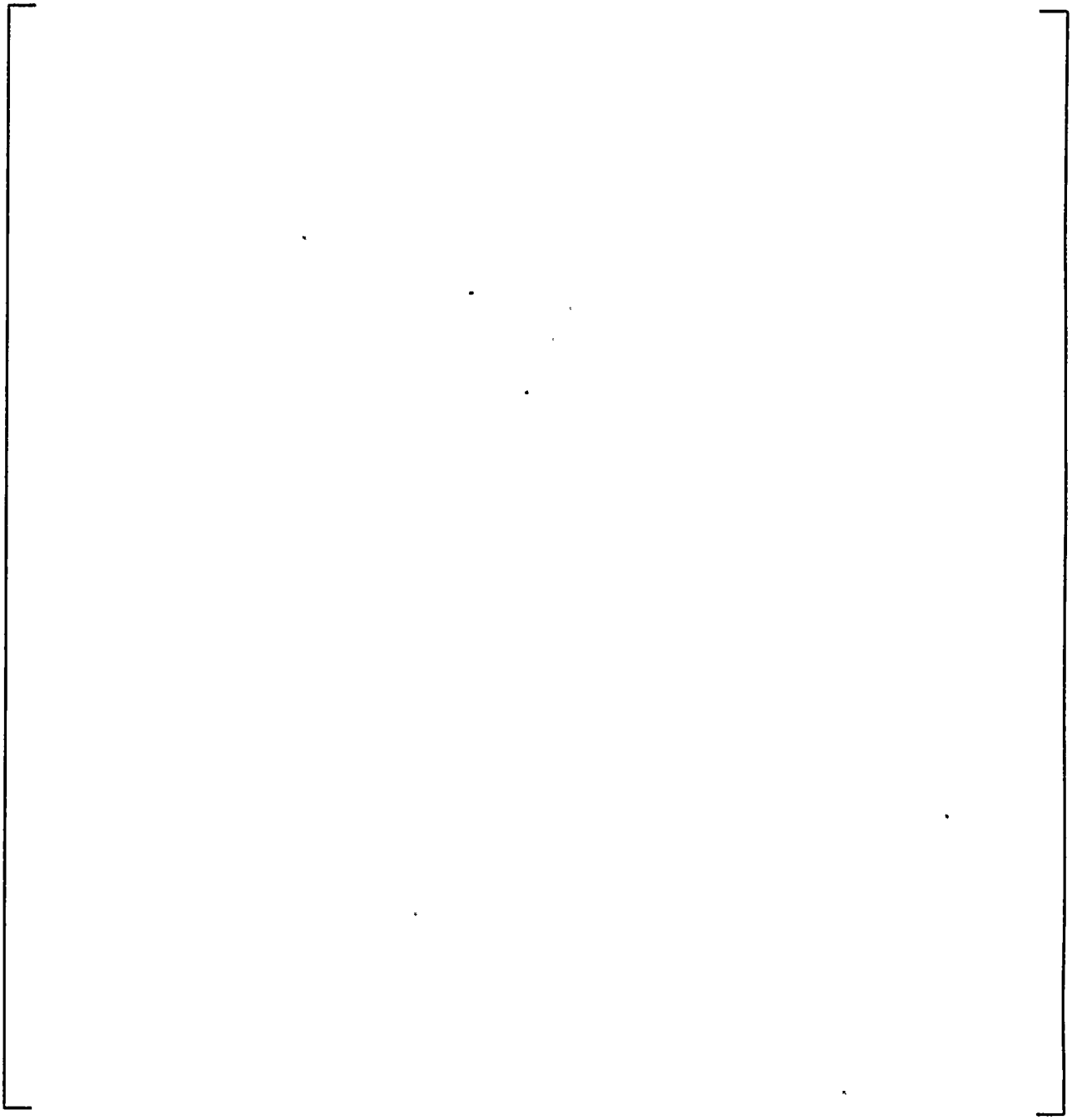

Figure 10-17. Revised Global Model
Location and Size of Detailed Plate Regions
Region 2

a,c

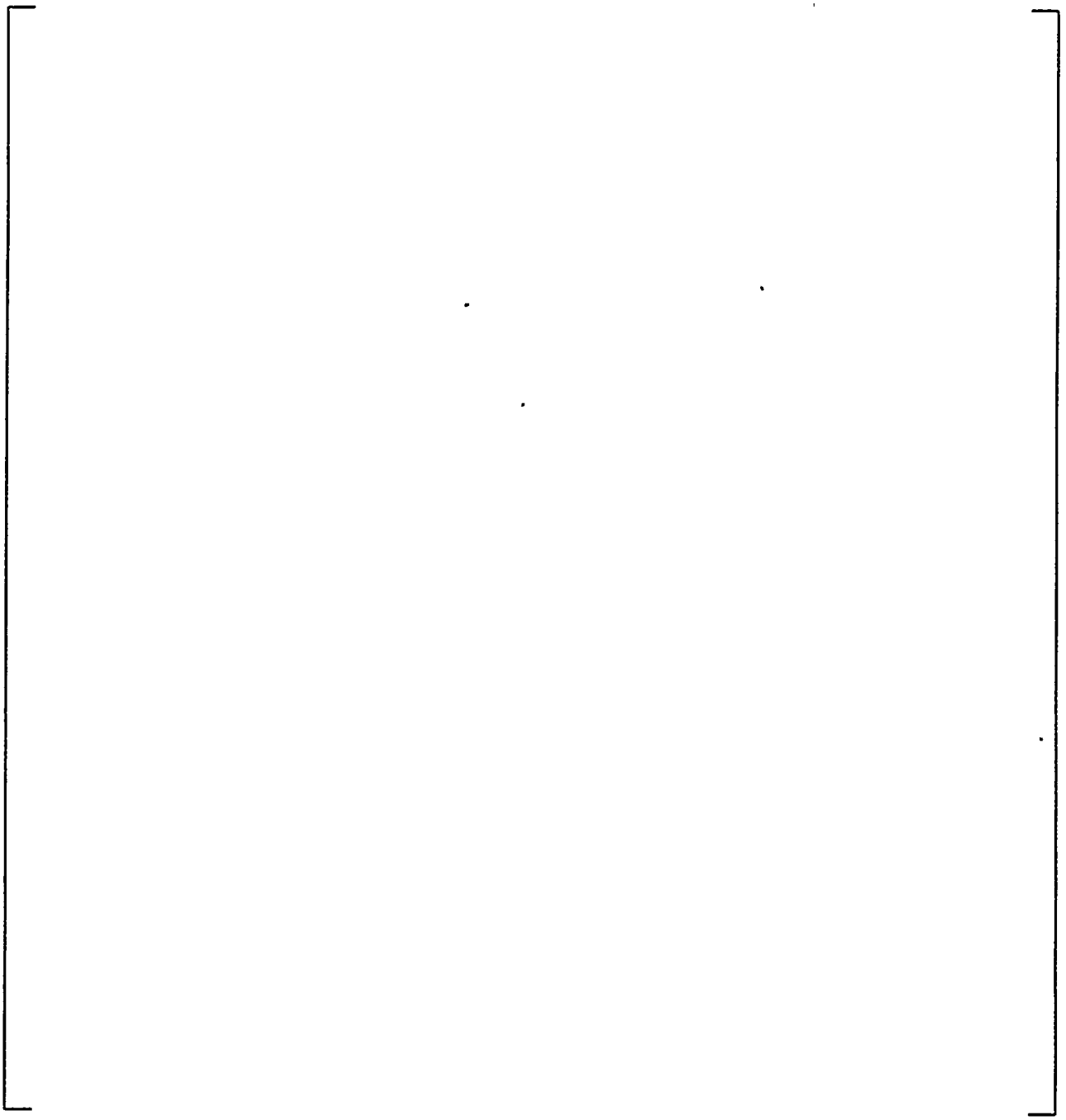

Figure 10-18. Displaced Geometry Plot
Quadrant 1 and 3 Support Conditions
Plate / Wrapper Interface - All DOF Coupled

a,c

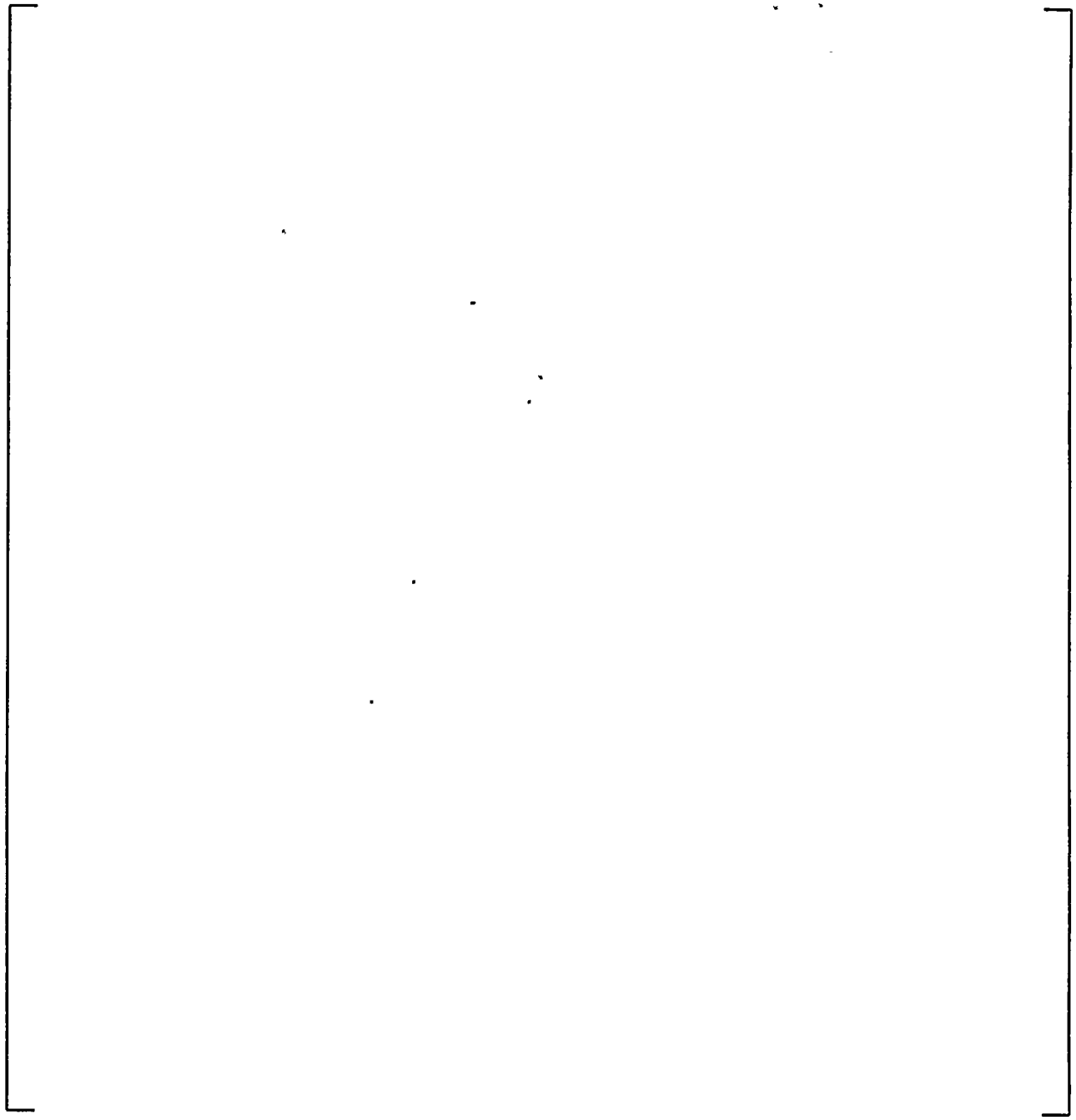

Figure 10-19. Displaced Geometry Plot
Enlarge View of Plates 6 and 7
Quadrant 1 and 3 Support Conditions
Plate / Wrapper Interface - All DOF Coupled

a,c

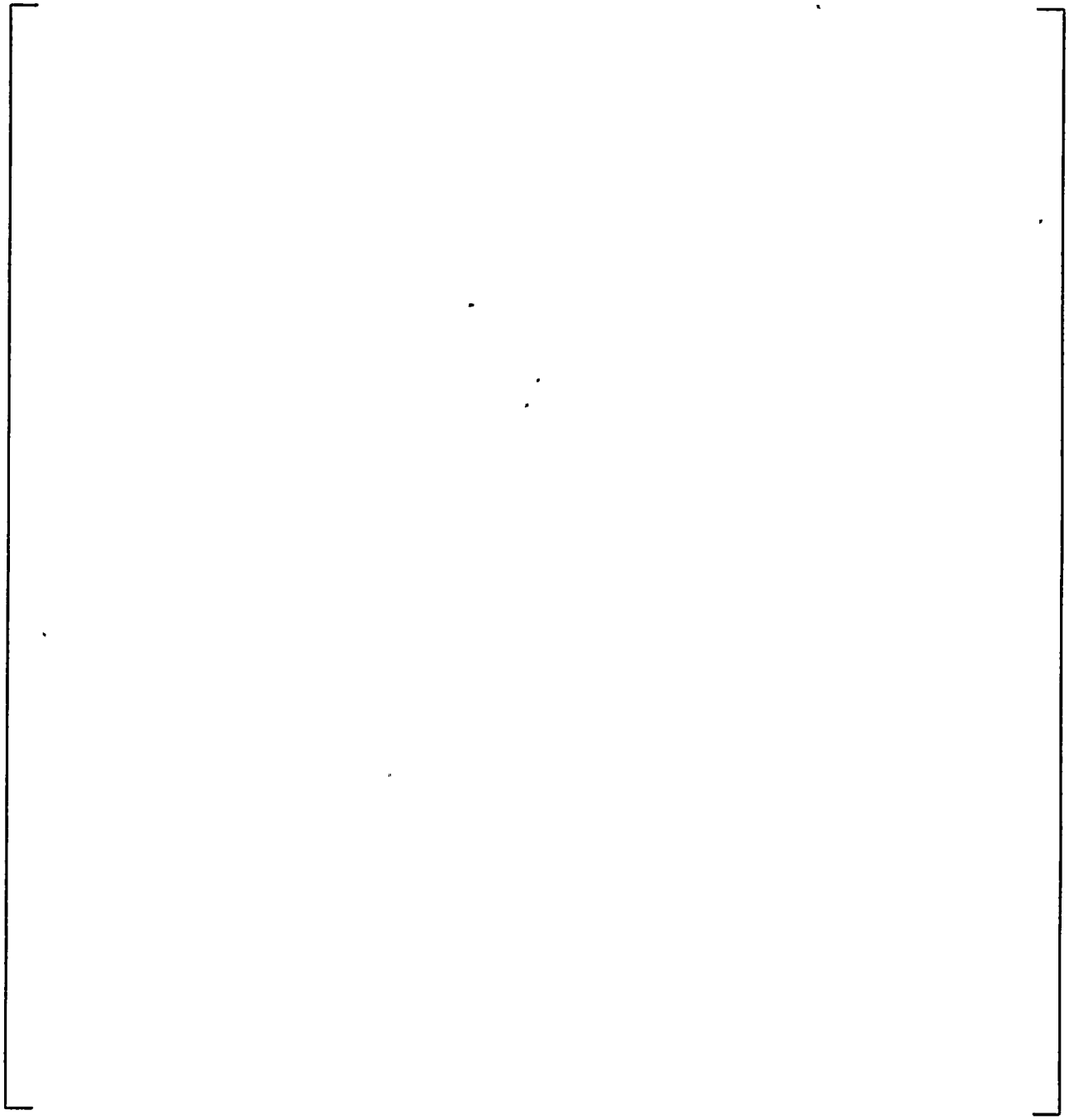

Figure 10-20. Displaced Geometry Plot
Quadrant 2 and 4 Support Conditions
Plate / Wrapper Interface - All DOF Coupled

a,c

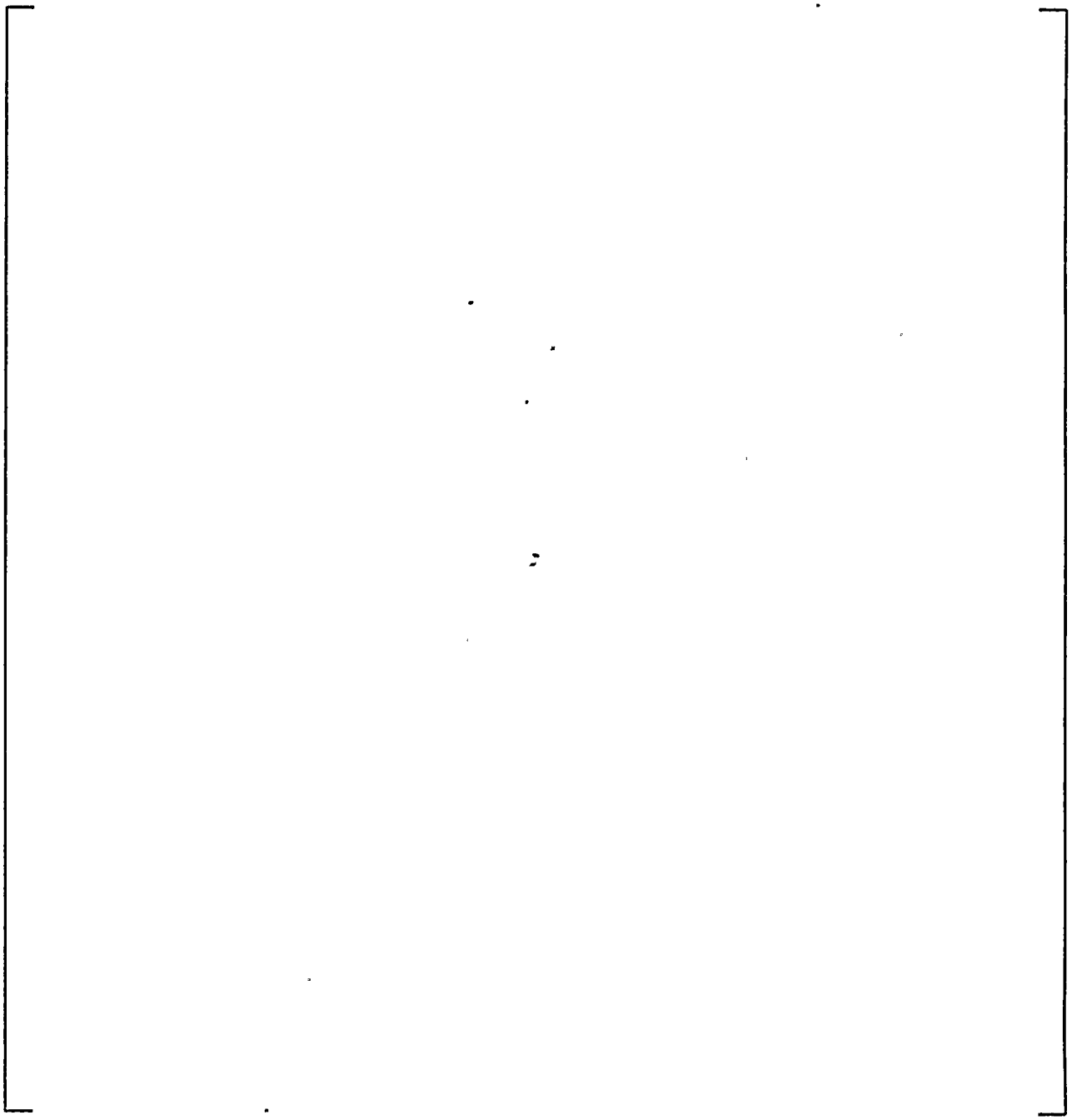

Figure 10-21. Displaced Geometry Plot
Enlarged View of Plates 6 and 7
Quadrant 2 and 4 Support Conditions
Plate / Wrapper Interface - All DOF Coupled

a,c

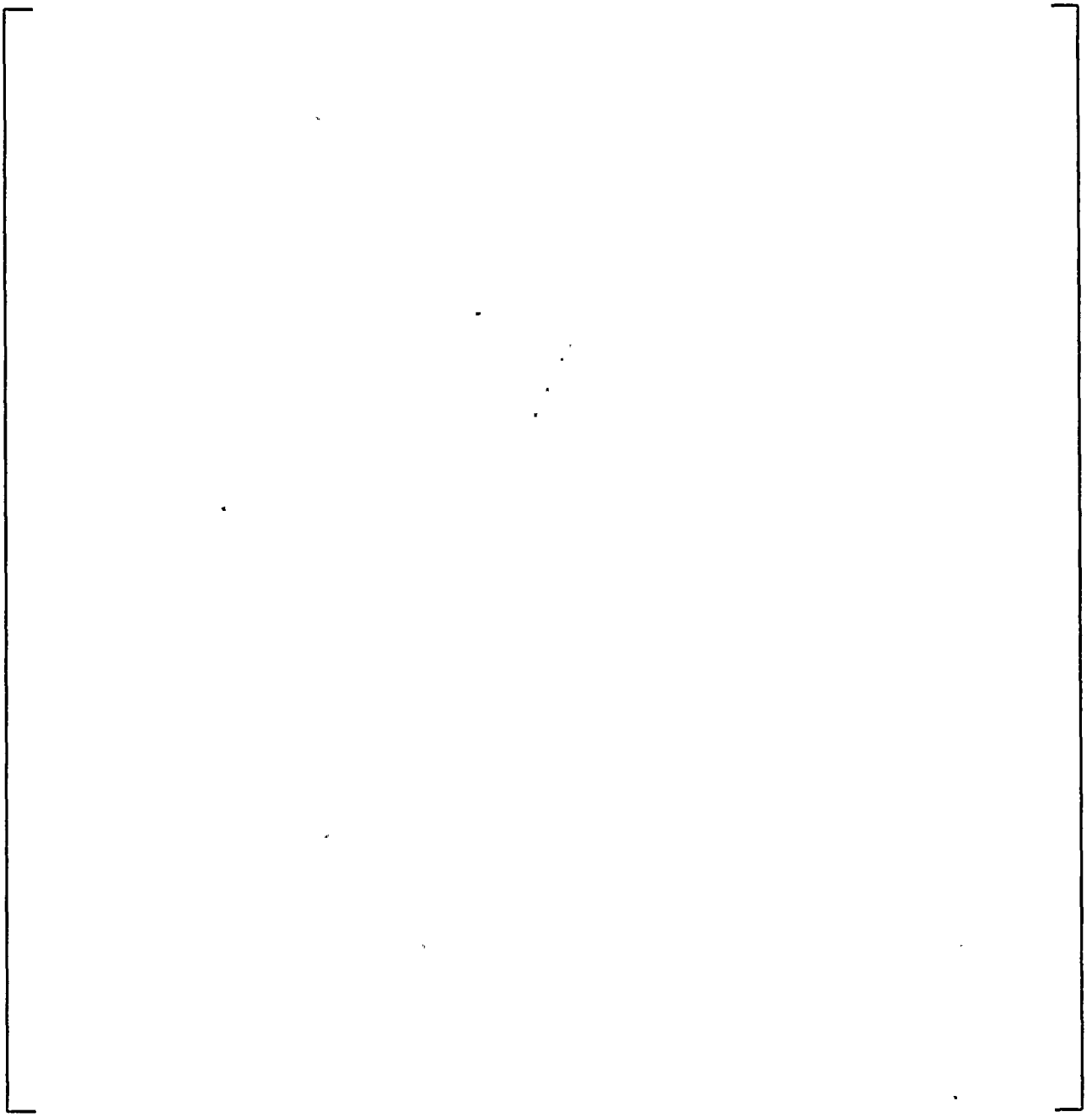

Figure 10-22. Tube Support Plate
Region Definition

a,c

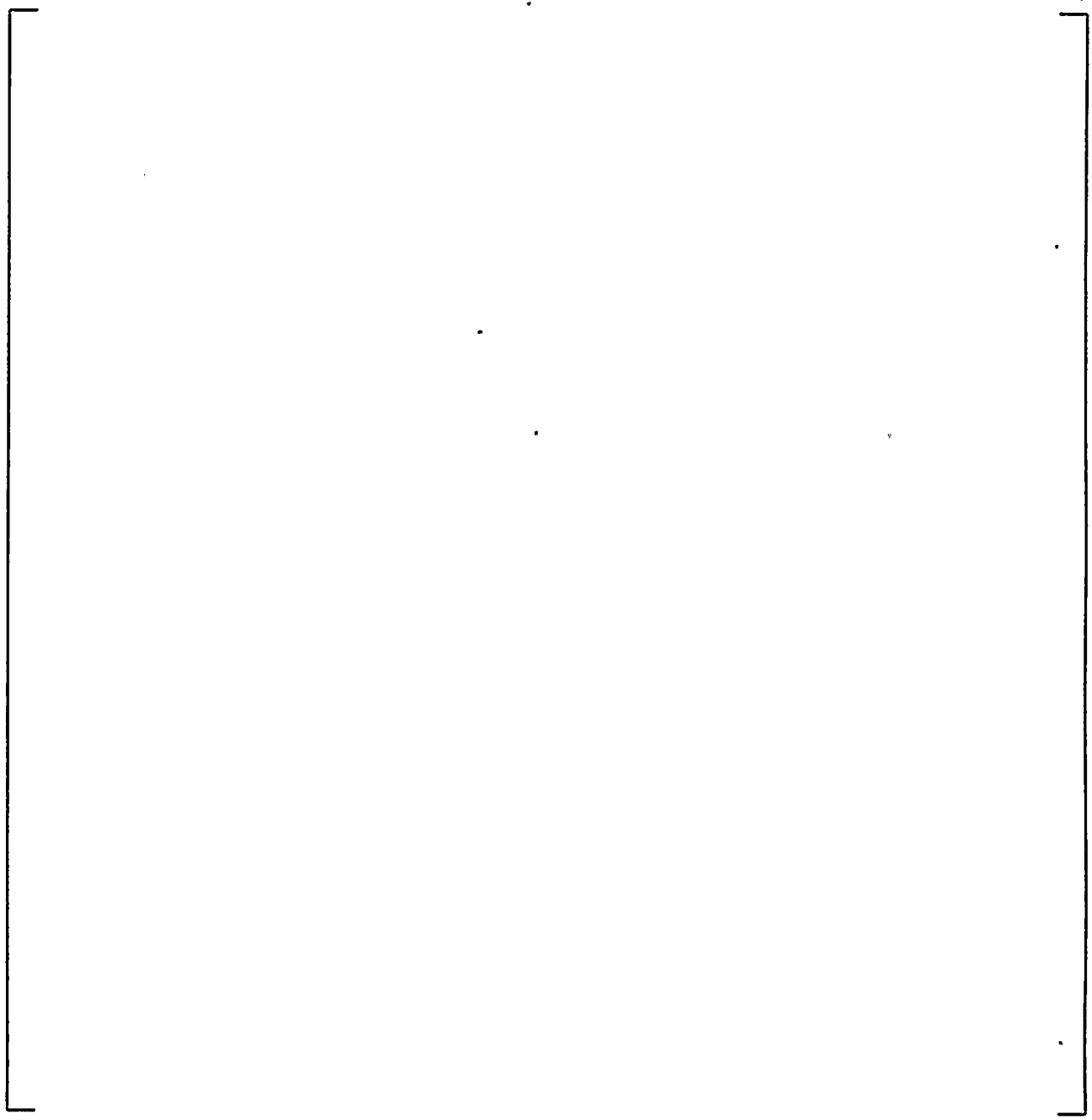

Figure 10-23. Location of Tubes That Exceed Breakaway Force
Plate 1 - Quadrant 1, 3

a,c

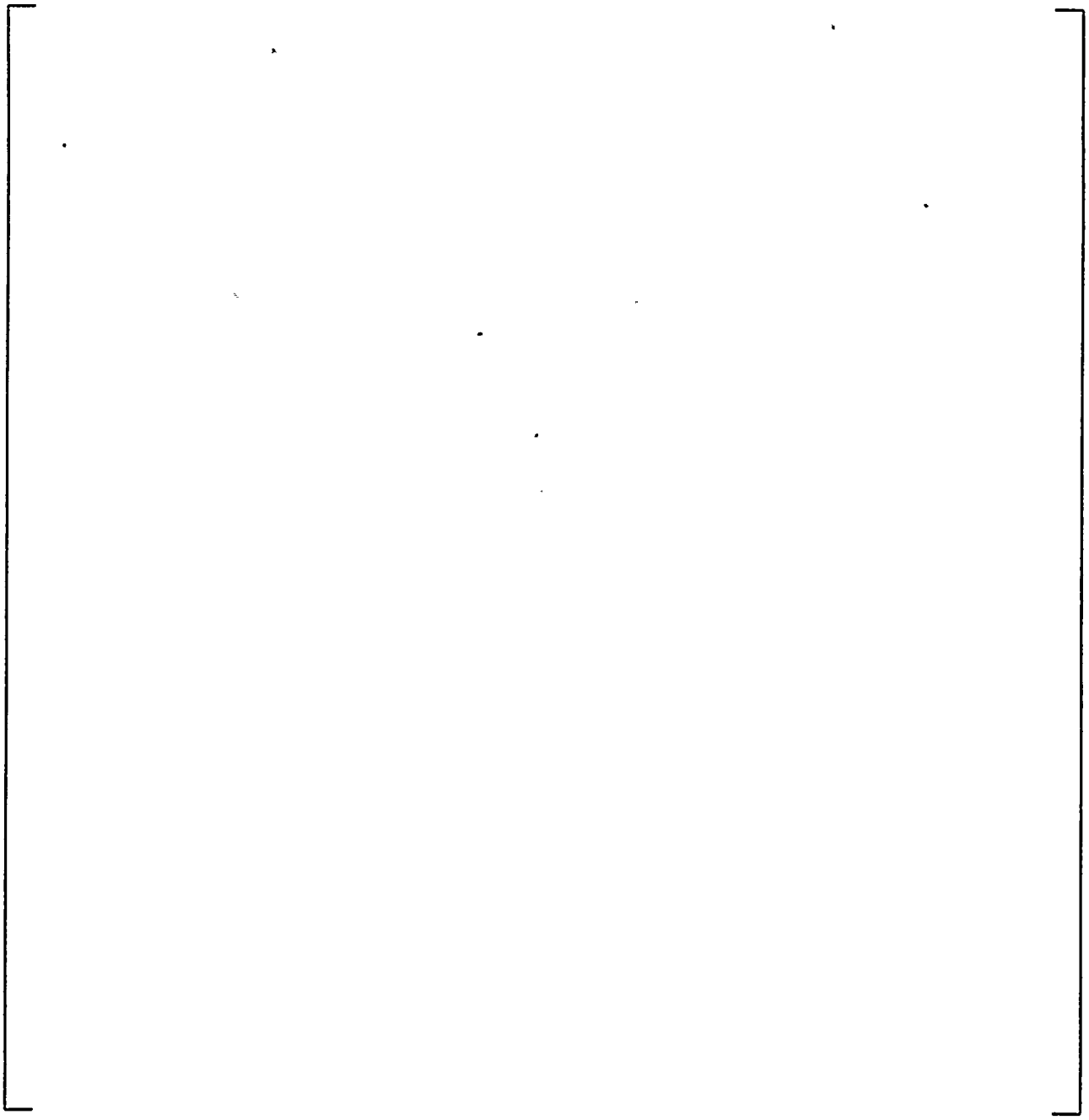

Figure 10-24. Location of Tubes That Exceed Breakaway Force
Plate 7 - Quadrant 1, 3

a,c

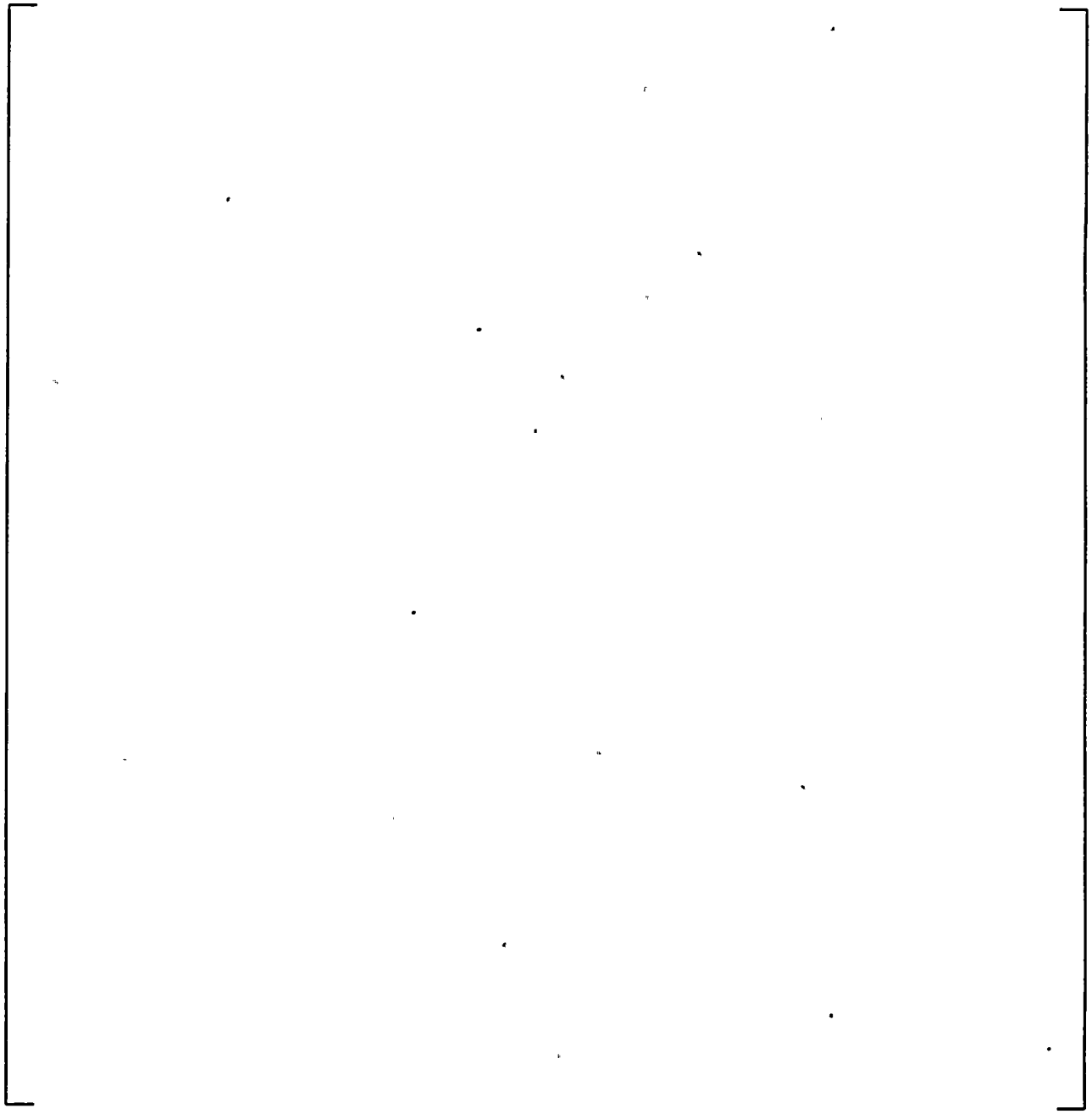

Figure 10-25. Location of Tubes That Exceed Breakaway Force
Plate 1 - Quadrant 2, 4

a,c

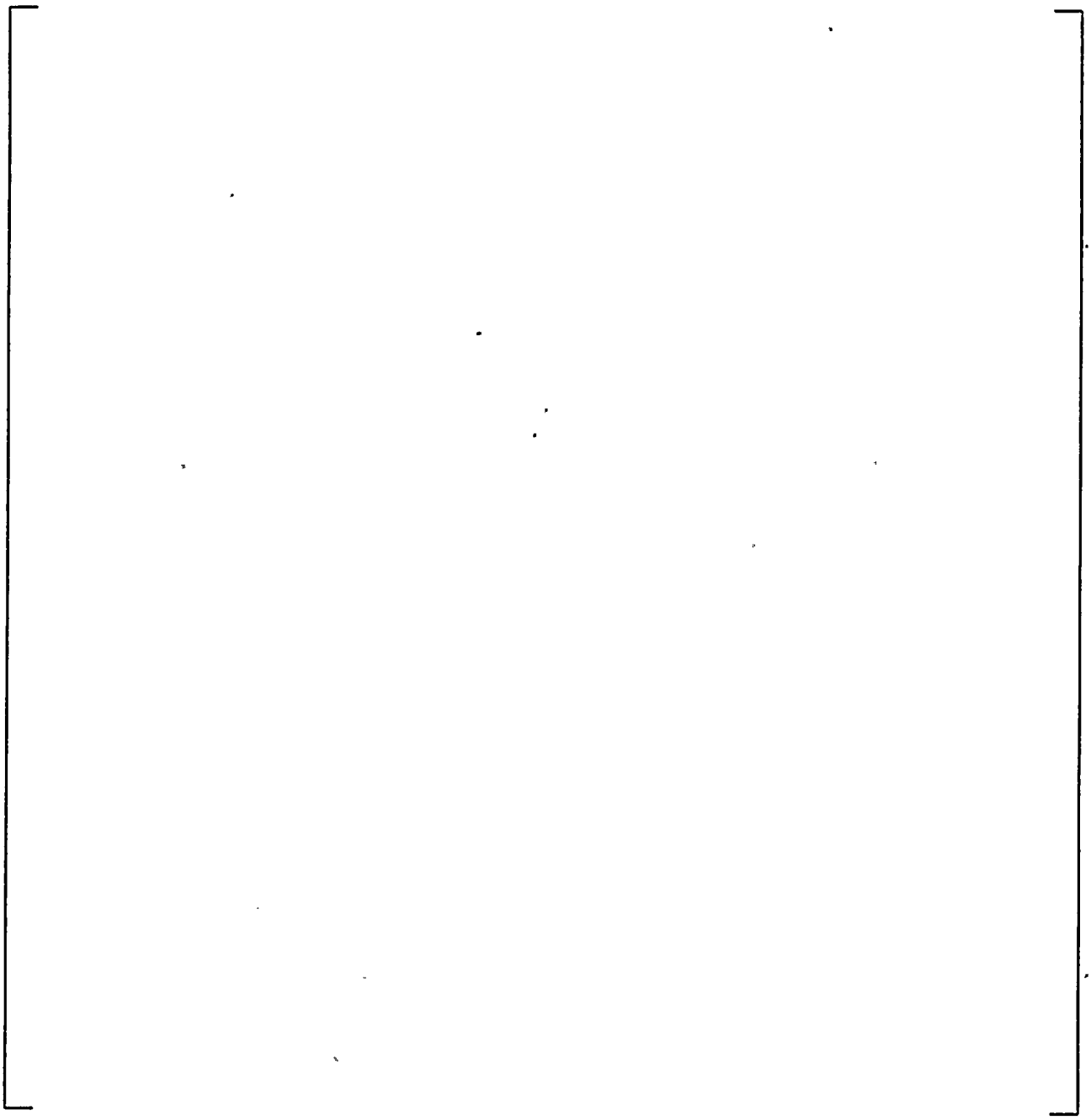

Figure 10-26. Location of Tubes That Exceed Breakaway Force Plate 6 - Quadrant 2, 4

a,c

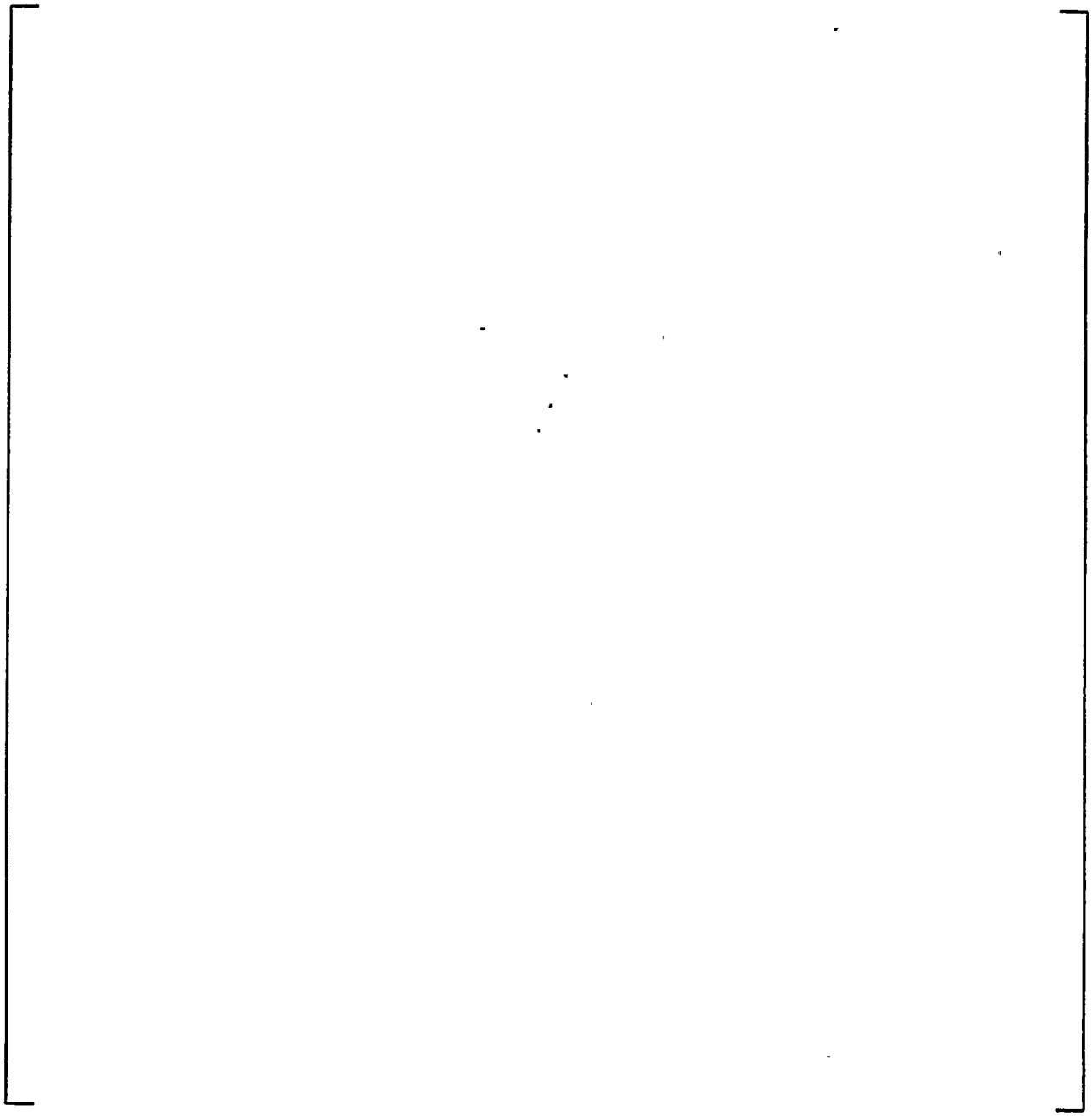

Figure 10-27. Location of Tubes That Exceed Breakaway Force
Plate 7 - Quadrant 2,4

a,c

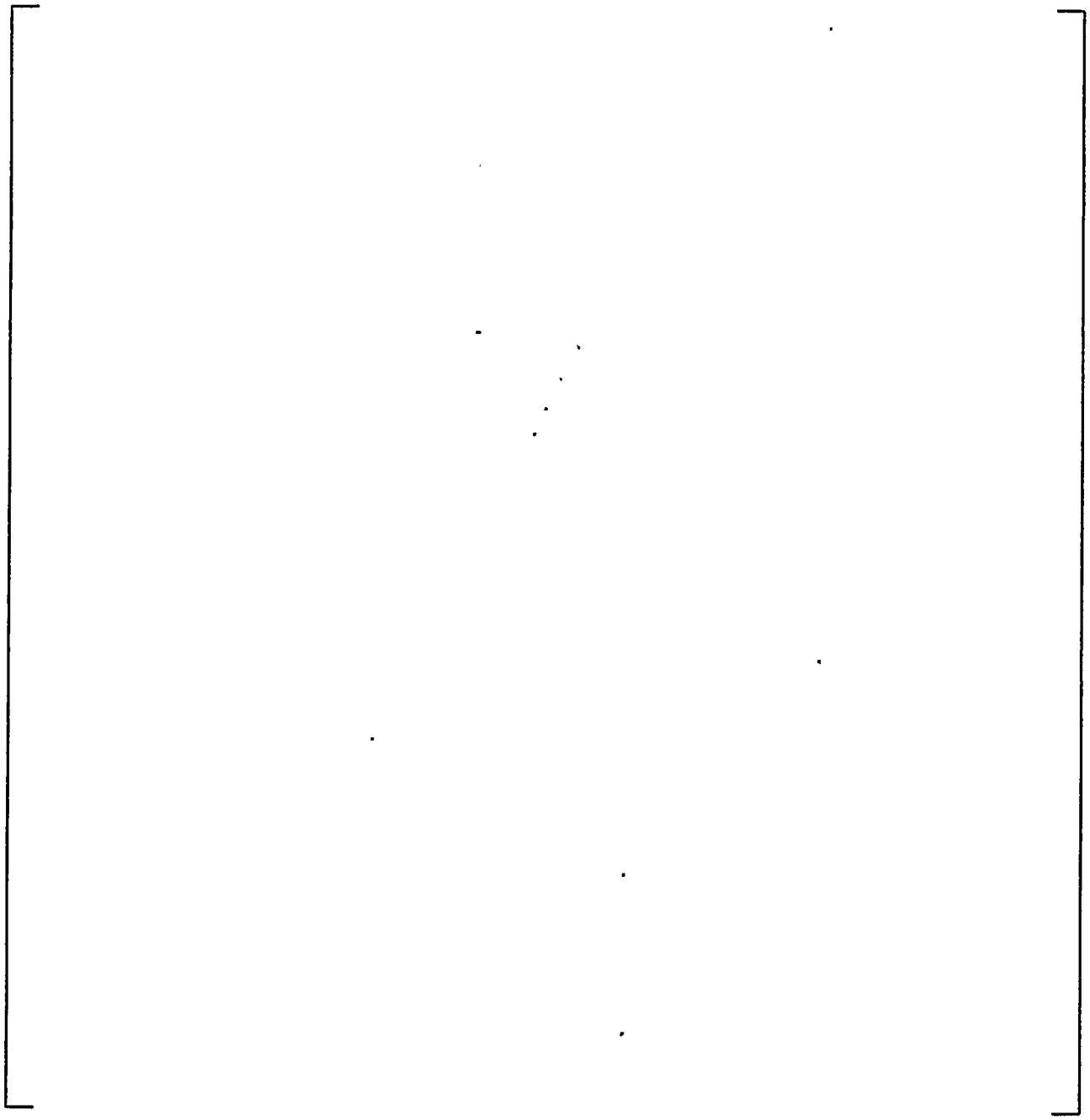

Figure 10-28. Distribution of Interface Forces
Plate 7 - Quadrant 1, 3 Support Conditions
Plate / Wrapper - All DOF Coupled

a,c

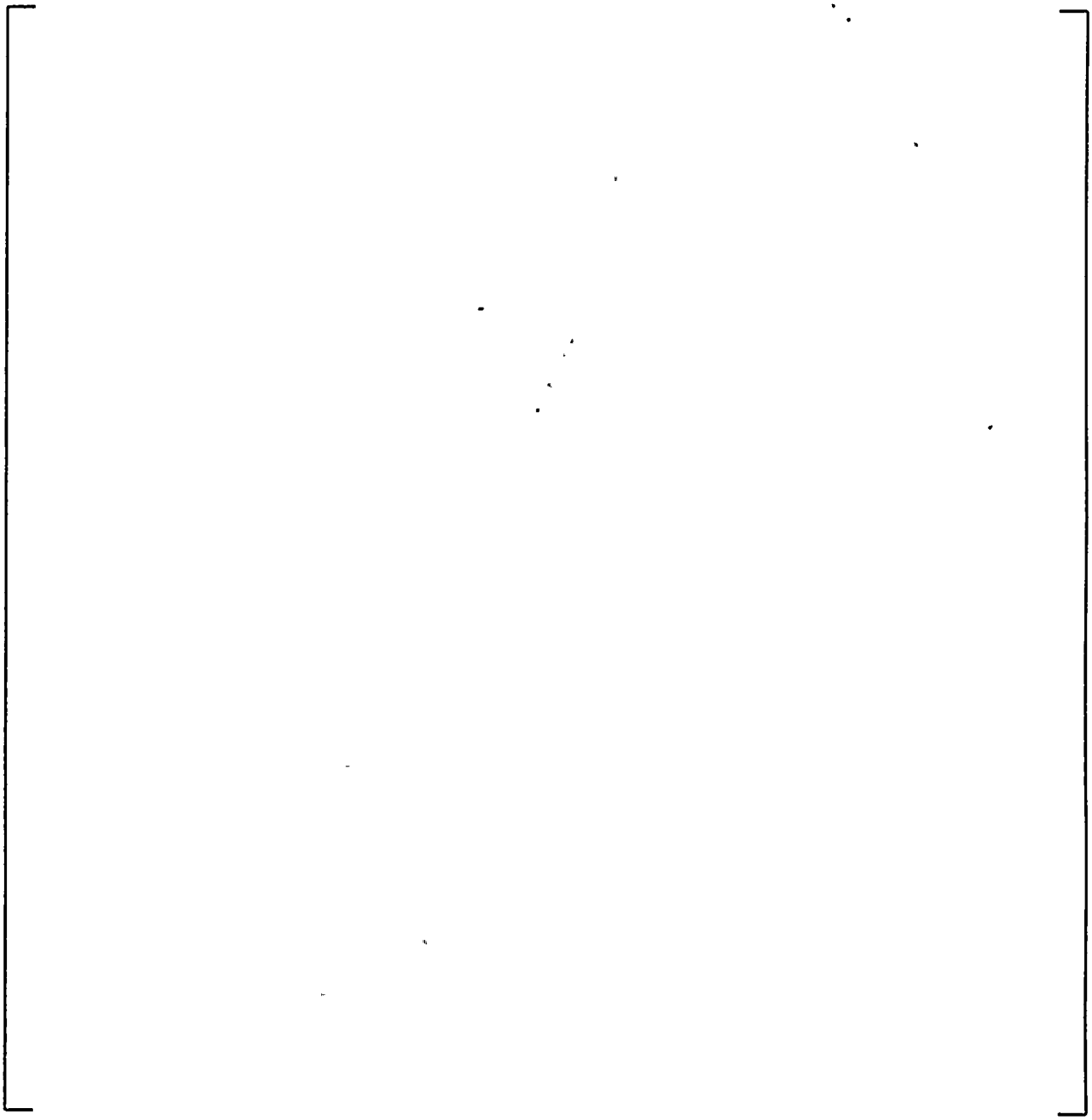

Figure 10-29. Distribution of Interface Forces
Plate 7 - Quadrant 1, 3 Support Conditions
Plate / Wrapper - Pinned Support

a,c

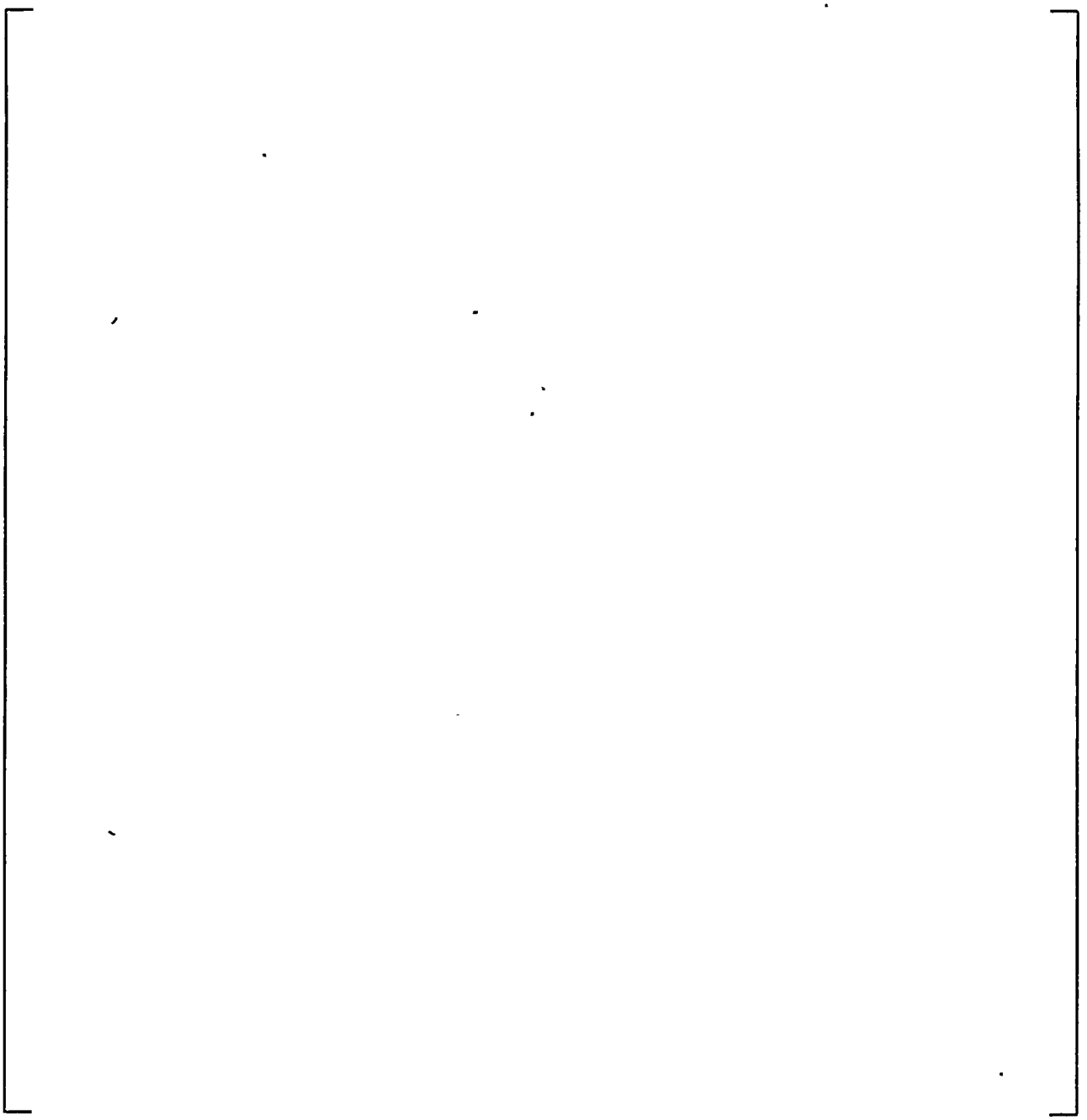

Figure 10-30. Distribution of Interface Forces
Plate 7 - Quadrant 2, 4 Support Conditions
Plate / Wrapper - All DOF Coupled

a,c

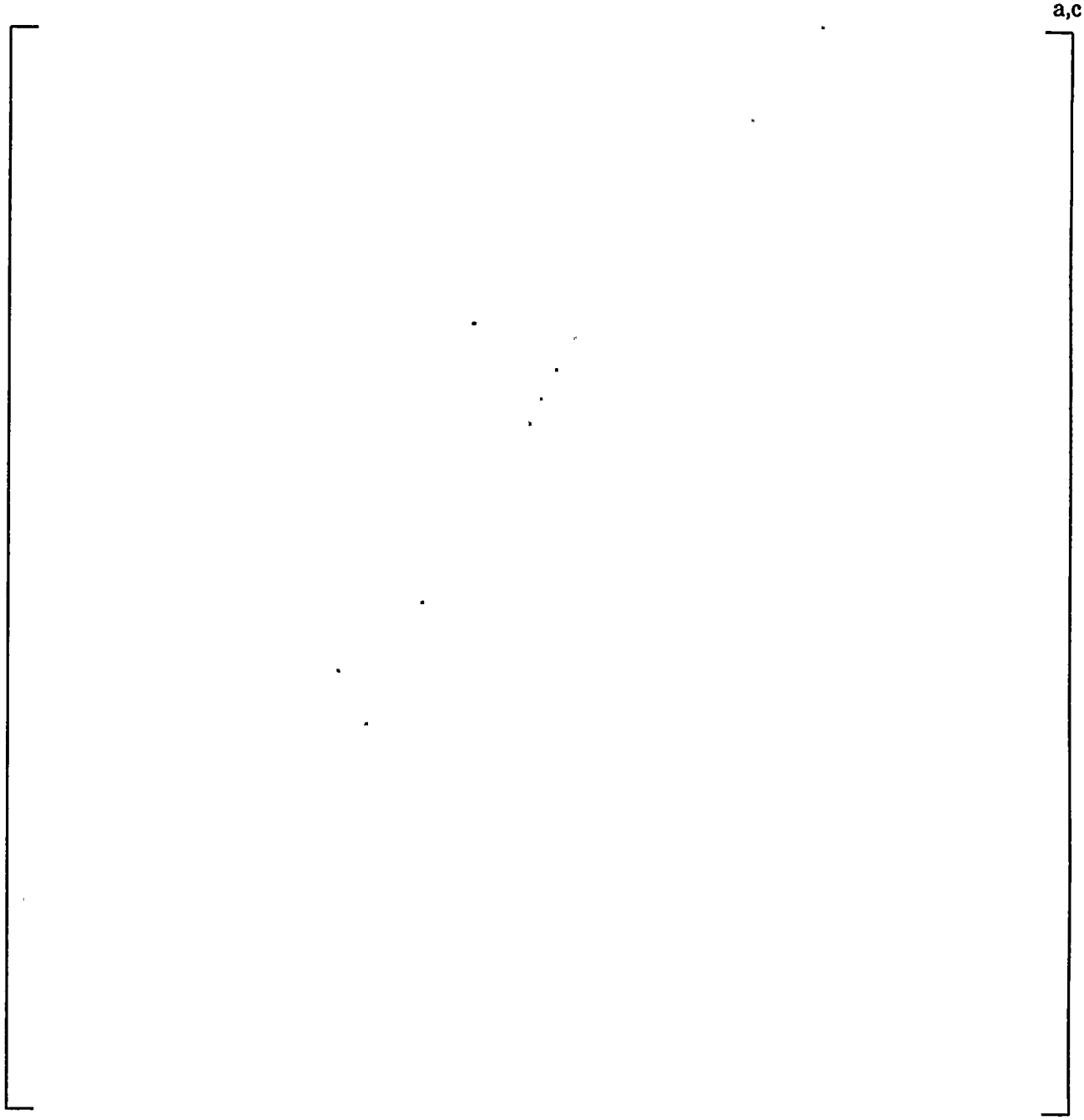

Figure 10-31. Distribution of Interface Forces
Plate 7 - Quadrant 2, 4 Support Conditions
Plate / Wrapper - Pinned Support

a,c

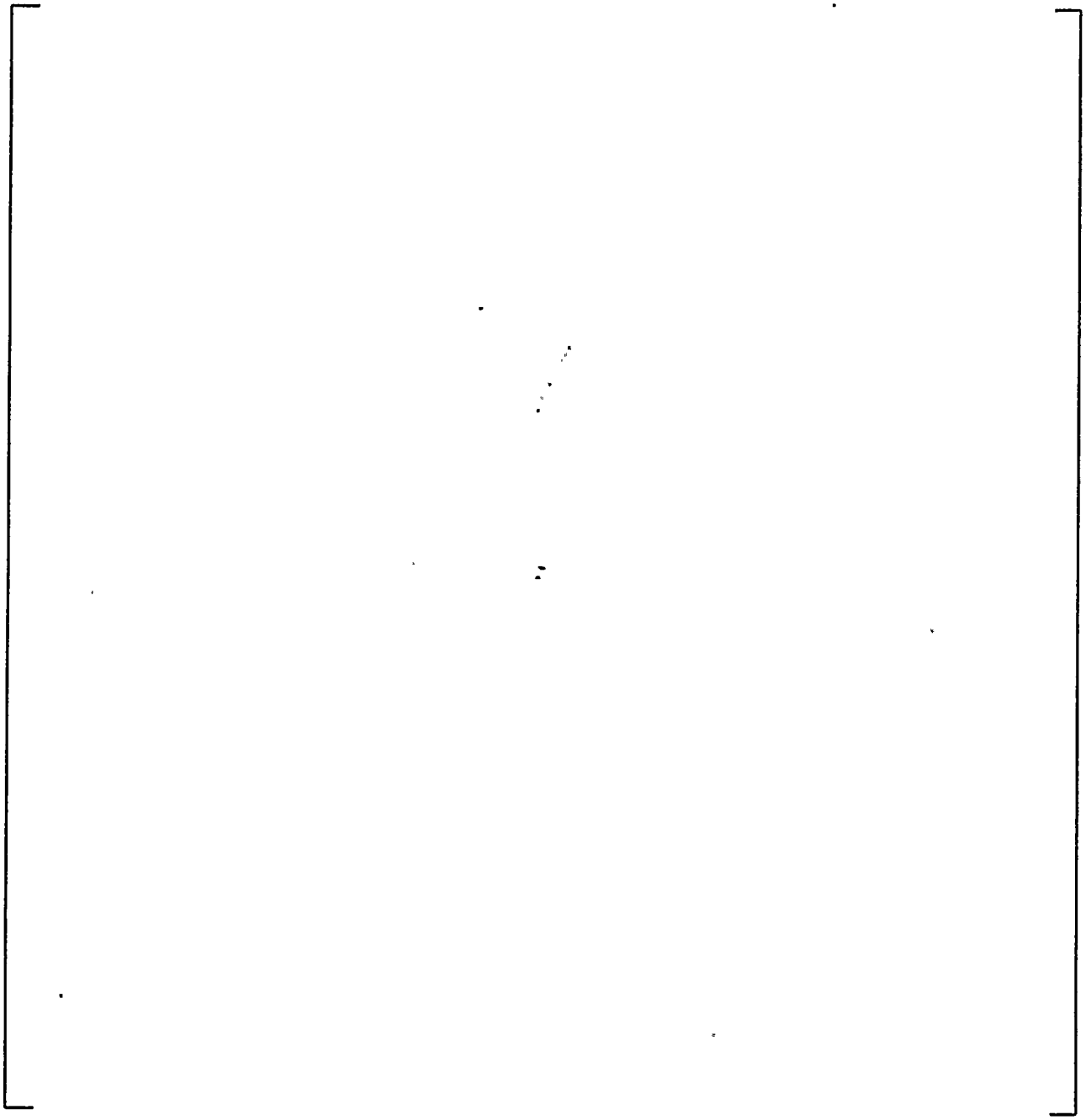

Figure 10-32. Stress Intensity Contour Plot
Plate 7 - Detail Region 1
Wedge at 12° Position

a,c

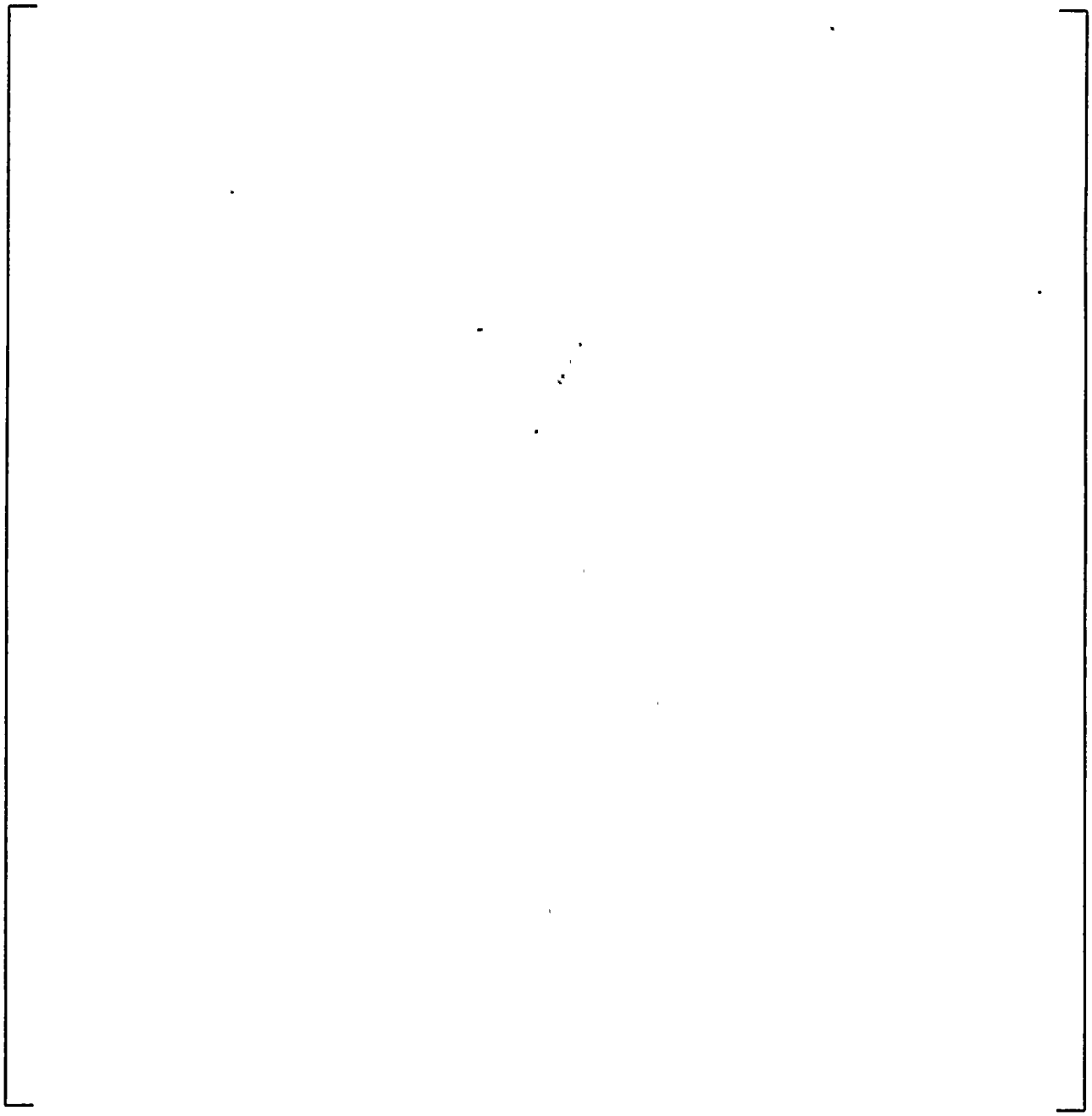

Figure 10-33. Stress Intensity Contour Plot
Plate 7 - Detail Region 2
Wedge at 48° (132°) Position

a,c

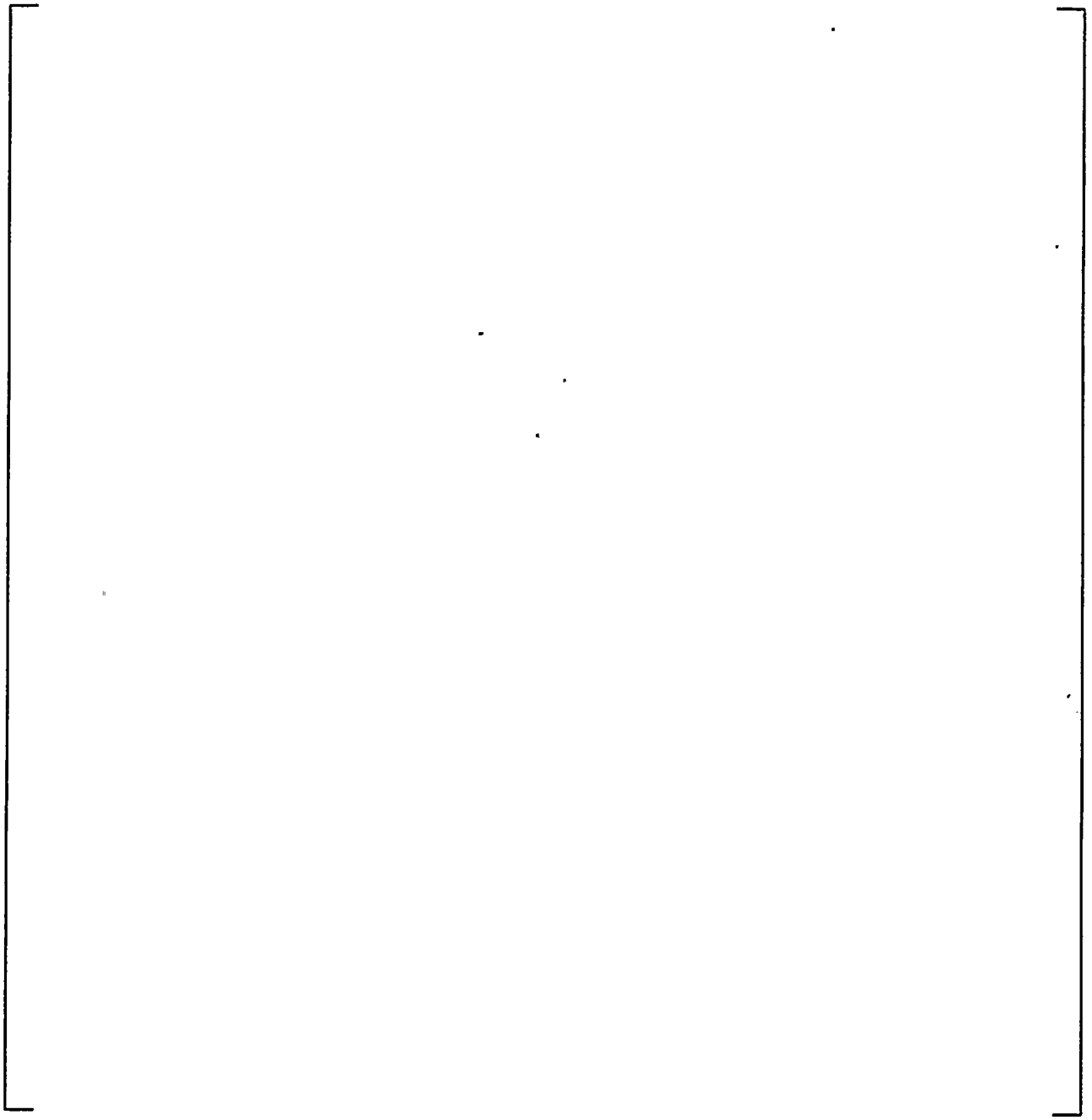

Figure 10-34. Stress Intensity Contour Plot
Plate 7 - Detail Region 3
Wedge at 72° Position

a,c

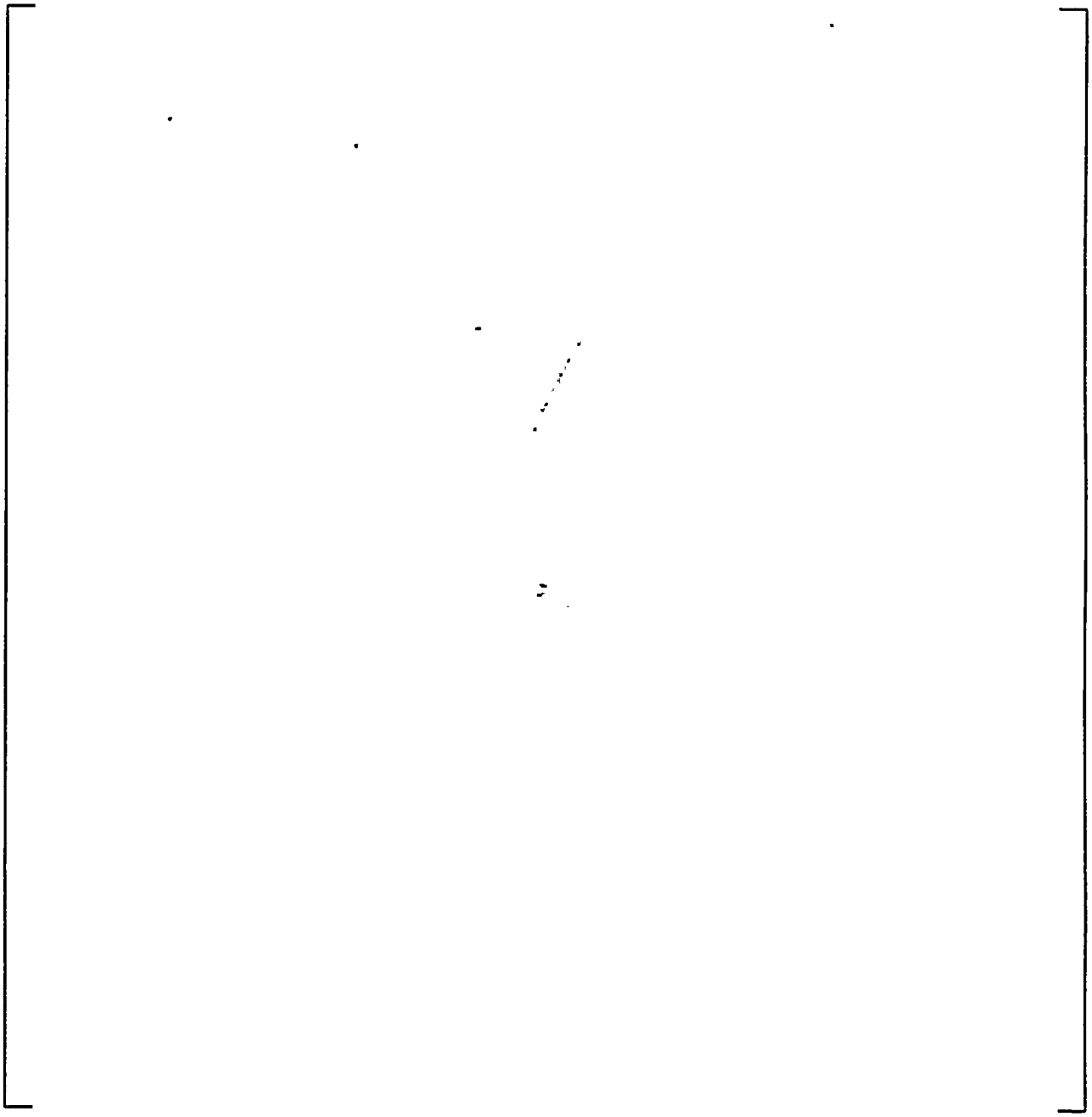

Figure 10-35. Stress Intensity Contour Plot
Plate 7 - Detail Region 3
Wedge at 78° (1" Vertical Bar) Position

a,c

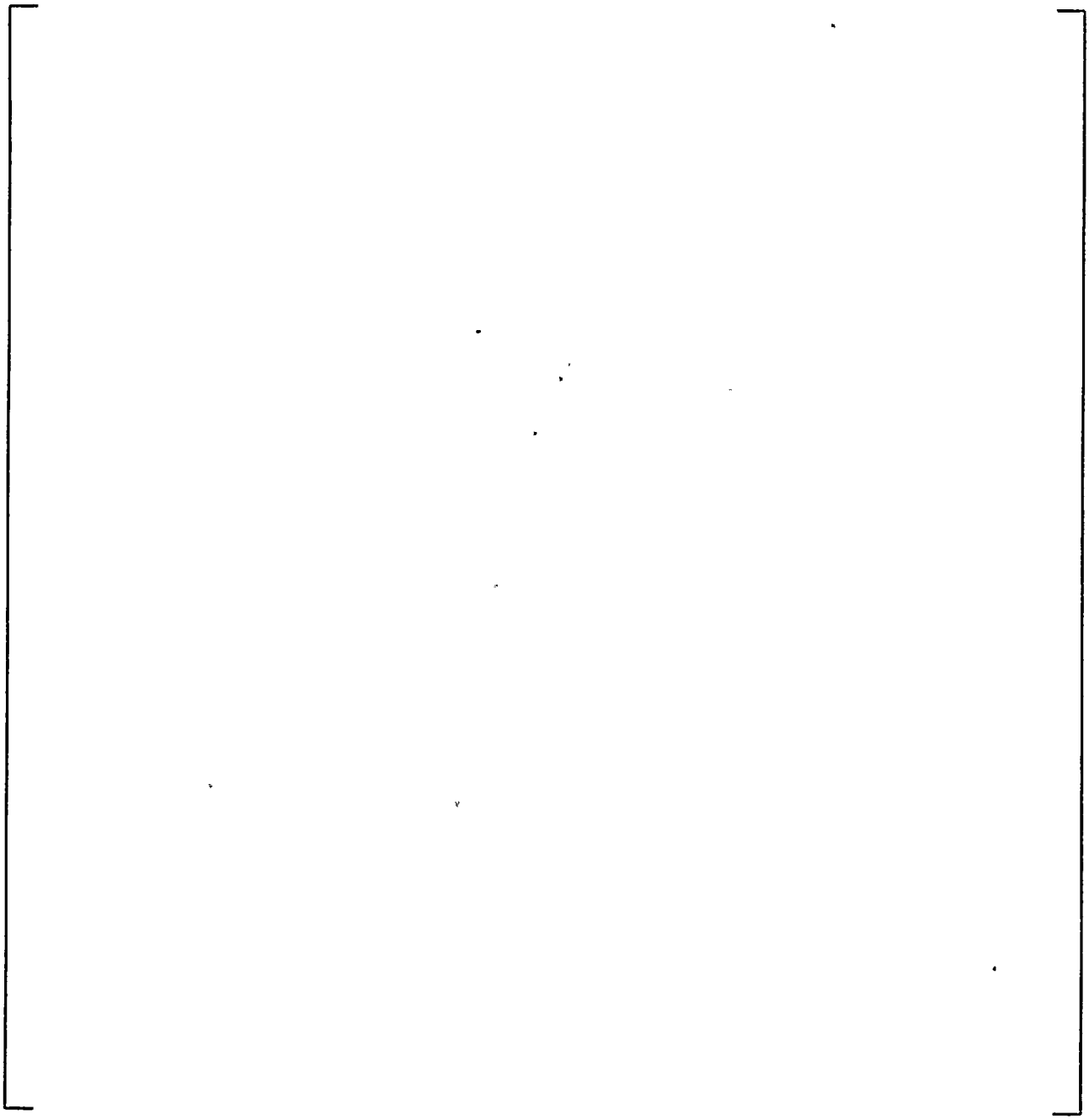

Figure 10-36. Stress Intensity Contour Plot
Plate 7 - Detail Region 4
Central Tierod Location